

Technical Report

TR-02-23

Pitting corrosion of copper

Further model studies

Claes Taxén

Swedish Corrosion Institute

August 2002

Svensk Kärnbränslehantering AB

Swedish Nuclear Fuel
and Waste Management Co
Box 5864

SE-102 40 Stockholm Sweden

Tel 08-459 84 00

+46 8 459 84 00

Fax 08-661 57 19

+46 8 661 57 19



Pitting corrosion of copper

Further model studies

Claes Taxén
Swedish Corrosion Institute

August 2002

Summary

The work presented in this report is a continuation and expansion of a previous study. The aim of the work is to provide background information about pitting corrosion of copper for a safety analysis of copper canisters for final deposition of radioactive waste. A mathematical model for the propagation of corrosion pits is used to estimate the conditions required for stationary propagation of a localised anodic corrosion process. The model uses equilibrium data for copper and its corrosion products and parameters for the aqueous mass transport of dissolved species.

In the present work we have, in the model, used a more extensive set of aqueous and solid compounds and equilibrium data from a different source. The potential dependence of pitting in waters with different compositions is studied in greater detail. More waters have been studied and single parameter variations in the composition of the water have been studied over wider ranges of concentration.

The conclusions drawn in the previous study are not contradicted by the present results. However, the combined effect of potential and water composition on the possibility of pitting corrosion is more complex than was realised. In the previous study we found what seemed to be a continuous aggravation of a pitting situation by increasing potentials. The present results indicate that pitting corrosion can take place only over a certain potential range and that there is an upper potential limit for pitting as well as a lower.

A sensitivity analysis indicates that the model gives meaningful predictions of the minimum pitting potential also when relatively large errors in the input parameters are allowed for.

Sammanfattning

Innehållet i denna rapport är en fortsättning på och utvidgning av en tidigare undersökning. Syftet med arbetet är att ta fram bakgrundsinformation om gropfrätning på koppar. Informationen skall användas för en säkerhetsanalys av de kopparkanistrar som man avser att slutförvara använt kärnbränsle i, ur korrosionssynpunkt.

En matematisk modell för gropfrätning används för att bestämma de förhållanden som måste råda för att en stationär tillväxt av en frätgrop skall kunna ske. Modellen använder jämviktsdata för koppar och dess korrosionsprodukter och parametrar för masstransport av lösta ämnen.

I denna fas av arbetet har vi i modellen använt en mer omfattande uppsättning av lösta och fasta ämnen än tidigare och utnyttjad en annan källa för jämviktsdata. Potentialberoendet hos gropfrätning i vatten med olika sammansättningar har studerats mer noggrant. Flera sammansättningar av vattnet har beaktats och gropfrätningens beroende av vattnets komponenter har studerats genom variationer i koncentrationen av komponenthalterna över större områden.

Slutsatserna från den föregående undersökningen motsägs inte av resultaten från denna studie. Dock finner vi att den kombinerade effekten av potential och vattensammansättning är mer komplicerad än vad som framgick tidigare. Tidigare fann vi att gropfrätning försvåras kontinuerligt av ökande potentialer. Beräkningar för större haltområden och större potentialvariationer tyder på att gropfrätning kan ske endast inom ett visst potentialområde. Det tycks finnas övre potentialgräns för gropfrätning så väl som en undre.

En känslighetsanalys visar att modellen ger meningsfulla förutsägelser av den lägsta potentialen för gropfrätning också om man tar hänsyn till relativt stora fel i ingående värden.

Table of contents

1	Background.....	1
2	The chemical system.....	2
3	The model and the calculations	7
4	Results and interpretation	8
4.1	Pitting corrosion at 25°C.....	8
4.1.1	The dependence on the potential	10
4.1.2	The influence of the chloride concentration.....	15
4.1.3	Influence of other water parameters	18
4.1.4	The influence of the sulphate concentration.....	18
4.1.5	The influence of the total carbonate concentration	20
4.1.6	The influence of the bulk pH.....	20
4.1.7	The influence of the concentration of dissolved oxygen.....	20
4.1.8	Pitting corrosion at 75°C	24
4.2	The existence of multiple solutions	24
4.3	Error analysis	25
5	Corrosion of copper in chloride rich waters	27
6	Discussion.....	31
6.1	Copper and water	31
6.2	Solid corrosion products on copper	31
6.3	Extrusion of corrosion products.....	32
7	Conclusions.....	34
8	References.....	35
9	Appendix 1. Selected result details for 25°C.....	36

1 Background

The work presented in this report is a continuation and expansion of Part I of this report. A summary of Part I had also been presented at a conference in Melbourne 1996 /1-1/. The aim of the work is to provide background information about pitting corrosion of copper for a safety analysis of copper canisters for final deposition of radioactive waste. In the previous study a mathematical model for the propagation of corrosion pits was described and used. The model uses equilibrium data and parameters for the aqueous mass transport of dissolved species. From the calculated profiles of concentration and mass transport we drew conclusions of the conditions required for stationary propagation of a localised anodic corrosion process.

In the present work we have used a more extensive set of aqueous and solid compounds. The thermodynamic data used are based on a compilation made by Puigdomenech and Taxén /2-1/ for the Swedish Nuclear Fuel and Waste Co. (SKB). The potential dependence of pitting in waters with different compositions is studied in greater detail. More waters have been studied and single parameter variations in the composition of the water has been studied over wider ranges of concentration. The work with validation of results by comparison to experimental data and case studies has continued. In the present work we also in greater detail, consider the implications of soil or rather compacted bentonite around the copper canisters.

2 The chemical system

Tables 2-1 through 2-4 show the aqueous and solid compounds considered.

Table 2-1. Mass transport and equilibrium data. Cuprous species at 25°C. Values of $\log_{10} k$ used in this study and in a previous study and from the compilation by Puigdomenech /2-1/ and from NIST /2-2/.

Cuprous species	$D \cdot 10^5$ (cm^2/s)	$\log_{10} k$				z	H^+	Cu^+	SO_4^{2-}	Cl ⁻
		Used '96	Puigd.'98	NIST	Used 98					
Cu^+		Component				1		1		
CuCl	1.2	2.7	2.10	3.1	2.10			1		1
CuCl_2^-	1.2	5.5	5.69	5.42	5.69	-1		1		2
CuCl_3^{2-}	1.2	5.7	5.02	4.75	5.02	-2		1		3
$\text{Cu}_2\text{Cl}_4^{2-}$	0.9	13.1		13	13	-2		2		4
$\text{CuOH}(\text{aq})$			-11.55		-		-1	1		
$\text{Cu}(\text{OH})_2^-$			-16.18		-	-1	-2	1		
$\frac{1}{2} \text{Cu}_2\text{O}(\text{s})$		0.8	0.74	0.70	0.74		-1	1		
$\text{CuCl}(\text{s})$		6.73	6.83	6.73	6.83			1		1
$\text{Cu}_2\text{SO}_4(\text{s})$			-1.95		-1.95			2	1	

Table 2-2. Mass transport and equilibrium data. Cupric species at 25°C. Values of $\log_{10} k$ used in this study and in a previous study and from the compilation by Puigdomenech /2-1/ and from NIST /2-2/.

Cupric species	$D \cdot 10^5$ (cm^2/s)	$\log_{10} k$				z	H^+	HCO_3^-	Cu^{2+}	SO_4^{2-}	Cl^-
		Used '96	Puigd.'98	NIST	Used 98						
Cu^{2+}	0.71	Component				2			1		
$\text{Cu}(\text{OH})^+$	0.70	-8	-7.96	-7.50	-7.96	1	-1		1		
$\text{Cu}(\text{OH})_2(\text{aq})$	0.70	-15.06	-16.24	-16.19	-16.24		-2		1		
$\text{Cu}(\text{OH})_3^-$	0.70		-26.70	-26.84	-26.70	-1	-3		1		
$\text{Cu}(\text{OH})_4^{2-}$	0.70		-39.60	-39.52	-39.60	-2	-4		1		
$\text{Cu}_2(\text{OH})_2^{2+}$	0.50	-10.36	-10.35	-10.16	-10.35	2	-2		2		
$\text{Cu}_3(\text{OH})_4^{2+}$	0.40		-21.10	-20.79	-21.10	2	-4		3		
CuCl^+	0.71	0.4	0.64	0.20	0.64	1			1	1	
$\text{CuCl}_2(\text{aq})$	0.71		0.61		0.61				1	2	
CuCl_3^-	0.71		-0.19		-0.19	-1			1	3	
CuCl_4^{2-}	0.71		-1.29		-1.29	-2			1	4	
$\text{CuCO}_3(\text{aq})$	0.65	-3.6	-3.56	-3.56	-3.56		-1	1	1		
CuHCO_3^+	0.65		1.80	1.80	1.80	1		1	1		
$\text{Cu}(\text{CO}_3)_2^{2-}$	0.62	-10.83	-10.45	-10.46	-10.45	-2	-2	2	1		
$\text{CuSO}_4(\text{aq})$	0.64	2.36	2.31	2.36	2.31				1	1	

Table 2-3. Equilibrium data. Cupric solids at 25°C. Values of $\log_{10} k$ used in this study and in a previous study and from the compilation by Puigdomenech /2-1/, from NIST /2-2/ and from Woods and Garrels /2-3/.

Cupric solids	$\log_{10} k$					H^+	HCO_3^-	Cu^{2+}	SO_4^{2-}	Cl^-
	Used 96	Puigd.'98	NIST	Woods	Used 98					
$\text{CuO}(\text{s})$	-7.62	-7.68	-7.64	-7.99	-7.68	-2		1		
$\text{Cu}(\text{OH})_2(\text{s})$	-8.64	-8.64	-8.67		-8.64	-2		1		
$\text{CuCO}_3(\text{s})$	-0.70	0.82	1.17		0.82	-1	1	1		
$\text{Cu}_2(\text{OH})_2\text{CO}_3(\text{s})$	-5.16	-5.03	-5.12	-4.38	-5.03	-3	1	2		
$\text{Cu}_3(\text{OH})_2(\text{CO}_3)_2(\text{s})$	-2.70	-3.75	-3.75	-1.98	-3.75	-4	2	3		
$\text{CuSO}_4(\text{s})$		-2.92			-2.92			1	1	
$\text{CuO}:\text{CuSO}_4(\text{s})$		-10.30			-10.30	-2		2	1	
$\text{Cu}_4(\text{OH})_6\text{SO}_4(\text{s})$	-15.36	-15.54	-15.22	-15.23	-15.54	-6		4	1	
$\text{Cu}_3(\text{OH})_4\text{SO}_4(\text{s})$	-8.79	-8.91		-8.87	-8.91	-4		3	1	
$\text{CuCl}_2(\text{s})$		-3.73			-3.73			1		2
$\text{Cu}_2(\text{OH})_3\text{Cl}(\text{s})$	-7.40	-7.50	-7.39	-7.11	-7.50	-3		2		1

Table 2-4. Mass transport and equilibrium data at 25°C. Species not containing copper. Values of $\log_{10} k$ used in this study and in a previous study and from the compilation by Puigdomenech /2-1/ and from NIST /2-2/.

Species not containing copper	D·10 ⁵ (cm ² /s)	log ₁₀ k				z								
		Used '96	Puigd.	NIST	Used 98	H ⁺	HCO ₃ ⁻	SO ₄ ²⁻	Cl ⁻	Ca ²⁺	Na ⁺			
H ⁺	9.31	Components				1	1							
HCO ₃ ⁻	1.18					-1		1						
SO ₄ ²⁻	1.06					-2			1					
Cl ⁻	2.03					-1				1				
Ca ²⁺	0.79					2						1		
Na ⁺	1.33					1								1
OH ⁻	5.27	-14.00	-14.00	-14.00	-14.00	-1	-1							
CO ₃ ²⁻	0.92	-10.33	-10.33	-10.33	-10.33	-2	-1	1						
CO ₂ (aq)	1.92	6.35	6.35	6.35	6.35		1	1						
NaCO ₃ ⁻	1.18			-9.70	-9.70	-1	-1	1			1			
NaHCO ₃ (aq)	1.18			-0.25	-0.25			1			1			
CaSO ₄	0.71	2.31		2.36	2.36				1	1				
CaCO ₃	0.71	-7.18		-7.13	-7.13		-1	1		1				
CaHCO ₃ ⁺	0.71	1.00		1.27	1.27	1		1		1				
NaSO ₄ ⁻	1.00	0.70		0.73	0.73	-1			1		1			
O ₂ (aq)	2.10	-75.28	-74.66		-74.66		-4*							
HSO ₄ ⁻	2.10		1.98		-		1		1					
CaCO ₃ (s)		-1.79		-1.85	-1.85		-1	1		1				
CaSO ₄ (s)		5.04		4.61	4.61				1	1				

* The activity of dissolved oxygen is calculated from the component activities using $\lg a(\text{O}_2(\text{aq})) = \lg k + 4 \lg a(\text{Cu}^{2+}) - 4 \lg a(\text{Cu}^+) - 4 \lg a(\text{H}^+)$ corresponding to the reaction: $\text{O}_2(\text{aq}) + 4 \text{Cu}^+ + 4 \text{H}^+ \rightarrow 4 \text{Cu}^{2+} + 2 \text{H}_2\text{O}$

Table 2-5. Mass transport and equilibrium data at 25°C. Redox processes. Values of $\log_{10} k$ used in this study and in a previous study and from the compilation by Puigdomenech /2-1/.

Redox Processes	D·10 ⁵ (cm ² /s)	log ₁₀ k			z		
		Used 96	Puigd. 98	Used 98	H ⁺	Cu ⁺	Cu ²⁺
e ⁻		-2.68	-2.83	-2.83		1	-1
Cu(s)		5.08	5.73	5.73		2	-1
O ₂ (aq)	2.1	-75.28	-74.66	-74.66	-4	-4	4
H ₂ (aq)		-	-8.75	-	2	2	-2

Table 2-6. Equilibrium data for 75°C

Cuprous species	log ₁₀ k		
	Used 96	Puigd.	Used 98
Cu⁺	Component		
CuCl	2.71	1.85	1.85
CuCl₂⁻	5.6	5.33	5.33
CuCl₃²⁻	4.96	4.49	4.49
Cu₂Cl₄²⁻	9.5	9.41	9.41
CuOH(aq)		-9.25	-
Cu(OH)₂⁻		-16.06	-
½ Cu₂O(s)	0.0	0.76	0.76
CuCl(s)	6.3	5.84	5.84
Cu₂SO₄(s)		-1.38	-1.38

Table 2-7. Equilibrium data for 75°C

Aqueous Cupric Species	log ₁₀ k		
	Used 96	Puigd.	Used 98
Cu²⁺	Component		
Cu(OH)⁺	-6.25	-6.9	-6.9
Cu(OH)₂(aq)	-11.95	-14.0	-14.0
Cu(OH)₃⁻		-23.88	-23.88
Cu(OH)₄²⁻		-36.35	-36.35
Cu₂(OH)₂²⁺	-8.8	-8.45	-8.45
Cu₃(OH)₄²⁺		-18.35	-18.35
CuCl⁺	1.16	0.97	0.97
CuCl₂(aq)		1.05	1.05
CuCl₃⁻		0.02	0.02
CuCl₄²⁻		-2.41	-2.41
CuCO₃(aq)	-1.6	-3.37	-3.37
CuHCO₃⁺		2.15	2.15
Cu(CO₃)₂²⁻	-7.68	-8.95	-8.95
CuSO₄(aq)	2.04	2.53	2.53

Table 2-8. Equilibrium data for 75°C

Cupric Solids	log ₁₀ k		
	Used 96	Puigd.	Used 98
CuO(s)	-6.0	-6.06	-6.06
Cu(OH) ₂ (s)	-7.18	-7.09	-7.09
CuCO ₃ (s)	0.13	1.44	1.44
Cu ₂ (OH) ₂ CO ₃ (s)	-3.37	-3.35	-3.35
Cu ₃ (OH) ₂ (CO ₃) ₂ (s)	-0.42	-1.52	-1.52
CuSO ₄ (s)		-0.89	-0.89
Cu ₄ (OH) ₆ SO ₄ (s)	-11.6	-11.01	-11.01
Cu ₃ (OH) ₄ SO ₄ (s)	-	-5.7	-5.7
CuCl ₂ (s)		-2.26	-2.26
Cu ₂ (OH) ₃ Cl(s)	-5.90	-5.65	-5.65

Table 2-9. Equilibrium data for 75°C

Species Not Containing Copper	log ₁₀ k					
	Used 96	Puigd.	Used 98			
H ⁺						
HCO ₃ ⁻	Components					
SO ₄ ²⁻						
Cl ⁻						
Ca ²⁺						
Na ⁺						
OH ⁻				-12.7	-12.71	-12.71
CO ₃ ²⁻				-10.17	-10.09	-10.09
CO ₂ (aq)				6.05	6.32	6.32
NaCO ₃ ⁻					-9.91	-9.91
NaHCO ₃ (aq)					-37	-37
CaSO ₄	2.48	2.42	2.42			
CaCO ₃	-6.53	-6.25	-6.25			
CaHCO ₃ ⁺	1.00	1.51	1.51			
NaSO ₄ ⁻	-	0.86	0.86			
O ₂ (aq)	-61.75	-59.80	-59.80			
HSO ₄ ⁻		2.68	-			
CaCO ₃ (s)	-1.08	-1.13	-1.13			
CaSO ₄ (s)	5.55	5.05	5.05			

Table 2-10. Equilibrium data for 75°C

Redox Processes	log ₁₀ k		
	Used 96	Puigd.	Used 98
e ⁻	-3.0	-3.01	-3.01
Cu(s)	5.0	3.75	3.75
O ₂ (aq)	-61.75	-59.80	-59.80
H ₂ (aq)	-	-6.02	-

3 The model and the calculations

Details of the model have been presented in Part I of this report and elsewhere /1-2/. In this phase of the work we have considered a larger number of chemical substances but the number of components is unchanged.

In this phase we have also calculated the local equilibria and mass transport rates with higher spatial resolution. Typically, about 1000-2000 elements were used whereas in the previous study about 300 elements was used from the undisturbed bulk solution to the corroding copper metal at the bottom of the pit.

4 Results and interpretation

4.1 Pitting corrosion at 25°C

Results from the calculations are illustrated using various types of diagrams. Figure 4-1 shows the results from a calculation of a corrosion pit in copper in a water with the composition in table 4-1.

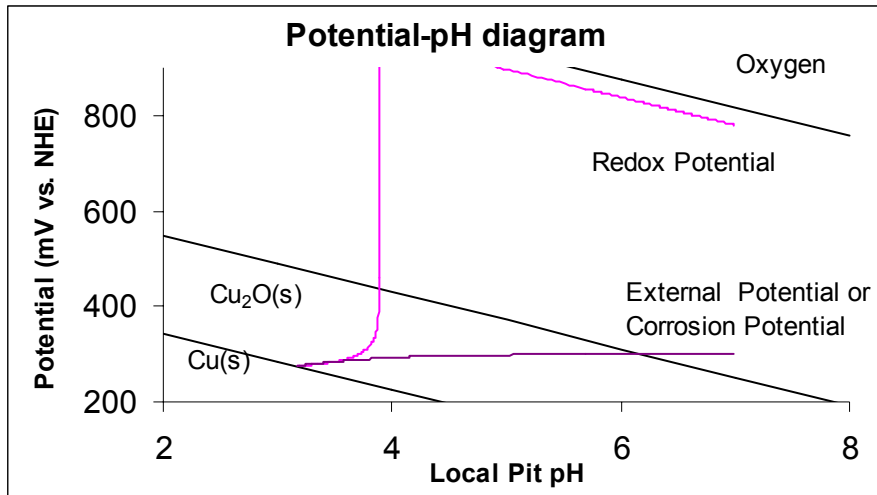


Figure 4-1. Conditions in a corrosion pit in copper illustrated in a potential-pH diagram. The straight lines indicate the relative stability of copper and its oxides and the reversible oxygen line at 1.0 atmospheres.

Table 4-1. Water composition used in the calculations in figure 4-1.

<i>Water composition</i>		
Temperature °C	25	
pH	7.0	
Total Concentrations	moles/litre	mg/litre
Chloride	0.0005	17.7
Sulphate	0.0040	384.0
Carbonate (mg CO ₃ ²⁻)	0.0012	69.0
Calcium	0.0005	21.6
Sodium	0.0086	197.1
Copper	1E-12	6.3E-08
Oxygen	5E-06	0.2

In the bulk of the solution outside the cavity, the redox potential is governed by the concentration of dissolved oxygen. Since we used a concentration much lower than that

which corresponds to saturation at 1.0 atmospheres partial pressure of oxygen the redox potential is slightly lower than the straight line. Further into the cavity the oxygen concentration decreases through reduction by aqueous cuprous species. At a pH slightly lower than pH 4, the oxygen concentration is practically zero. Significant concentrations of aqueous cuprous species exist below this pH. The redox potential continues to decrease until the stability region of copper metal is encountered. The local redox potential at the corroding copper metal at the bottom of the pit is reflected in a slightly higher measurable potential outside the cavity. The small slope of the line indicating the external potential or corrosion potential is caused by the successive additions of the local iR -drops and diffusion potentials caused by current transport and concentration gradients.

Figure 4-2 shows the fraction of the oxidised copper which is transported outwards as dissolved species. In this water and at this potential we find that the transport of cuprous species is negligible and the aqueous transport of copper is almost exclusively in the form of cupric species. At about pH 5.5 saturation and precipitation of cupric solids occurs. This is shown by a decrease in the transported fraction as higher pH values are encountered.

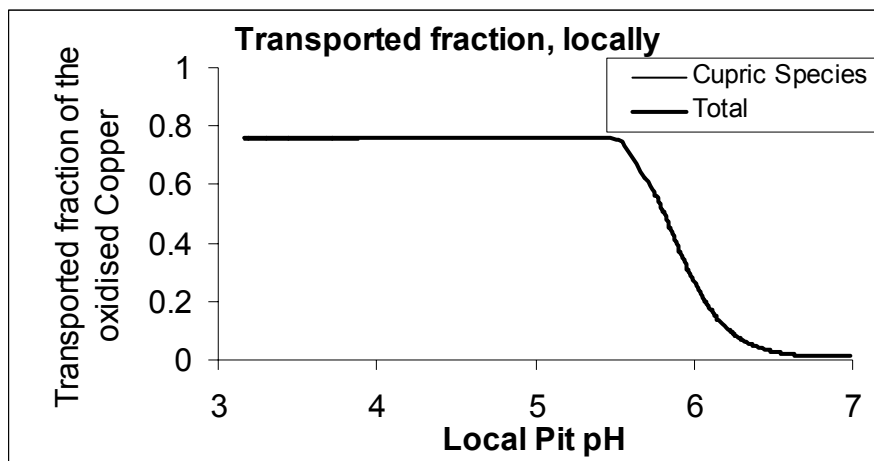


Figure 4-2. Conditions in a corrosion pit in copper illustrated as the fraction of the oxidised copper which is transported outwards as dissolved species as function of the local pH in the pit.

Figure 4-3 shows log activity of the cuprous and cupric solids considered as function of the local pH in the cavity. At the higher pH range, there is precipitation of malachite, $\text{Cu}_2(\text{OH})_2\text{CO}_3(\text{s})$, and over a narrow pH range around pH 5.5 of brochantite, $\text{Cu}_4(\text{OH})_6\text{SO}_4(\text{s})$. Cuprous oxide, $\text{Cu}_2\text{O}(\text{s})$, reaches saturation at the lowest pH whereas cuprous chloride, $\text{CuCl}(\text{s})$, does not reach saturation and does not form in this particular corrosion pit. Not shown in the diagram is the activity of metallic copper which reaches unity at the lowest pH.

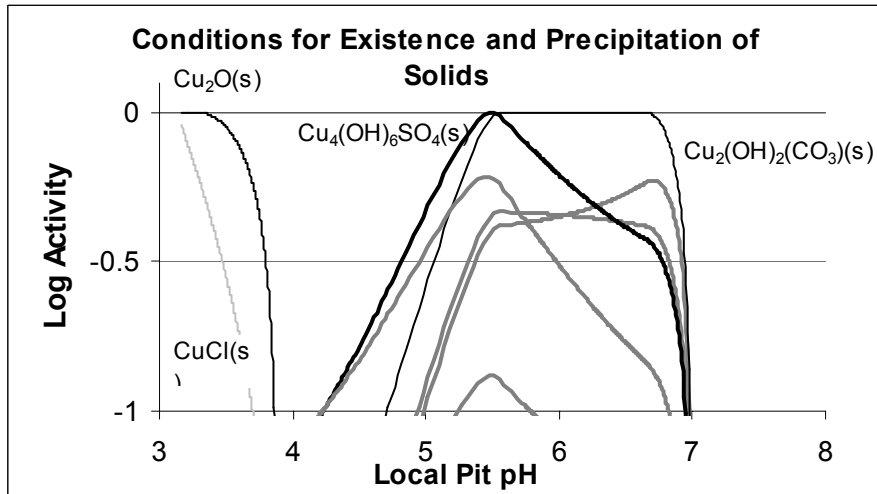


Figure 4-3. Conditions in a corrosion pit in copper illustrated as log activity of the cuprous and cupric solids considered, as function of the local pH in the cavity.

Figure 4-4 shows the end products of the oxidised copper. In this particular pit, only about two percent of the oxidised copper leaves the site of the pit as aqueous species. The main part will form a crust of cupric basic salts, malachite and brochantite outside the cavity and about 24% will form cuprous oxide, mainly inside the cavity.

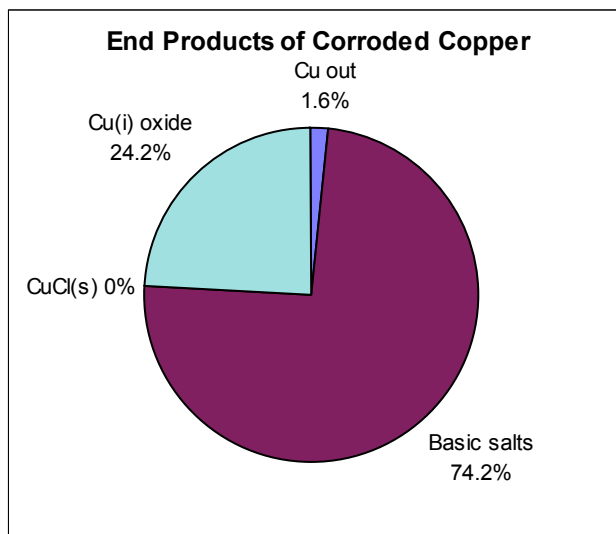


Figure 4-4. End products of the oxidised copper

4.1.1 The dependence on the potential

The corrosion pit illustrated in figures 4-1 to 4-4 is represented as a single point in figure 4-5. The diagram shows the distribution of the corrosion products into a solid fraction and a dissolved fraction at the bottom of a corrosion pit. The curve shows the fraction of the oxidised copper which is formed as dissolved species, as function of the

potential in the bulk solution outside the cavity. If this fraction is higher than 0.4 an occluded cell can be maintained so that there is an aqueous solution between the copper metal and deposited corrosion products. If the fraction of the oxidised copper that forms solid phases i.e. $\text{Cu}_2\text{O}(\text{s})$, at the corroding copper surface is too high, the necessary aqueous transport of mass and charge would be obstructed and the pitting process would cease.

Table 4-2 shows the derivation of the limiting value of the transported fraction. 60% of the molar contents of copper in a volume of copper metal would completely fill that volume in the form of $\text{Cu}_2\text{O}(\text{s})$. There is an excess of copper of about 40%. If the product instead is $\text{CuCl}(\text{s})$ and no $\text{Cu}_2\text{O}(\text{s})$ then there is an excess of copper of about 70% which must be transported away so that aqueous mass transport is possible.

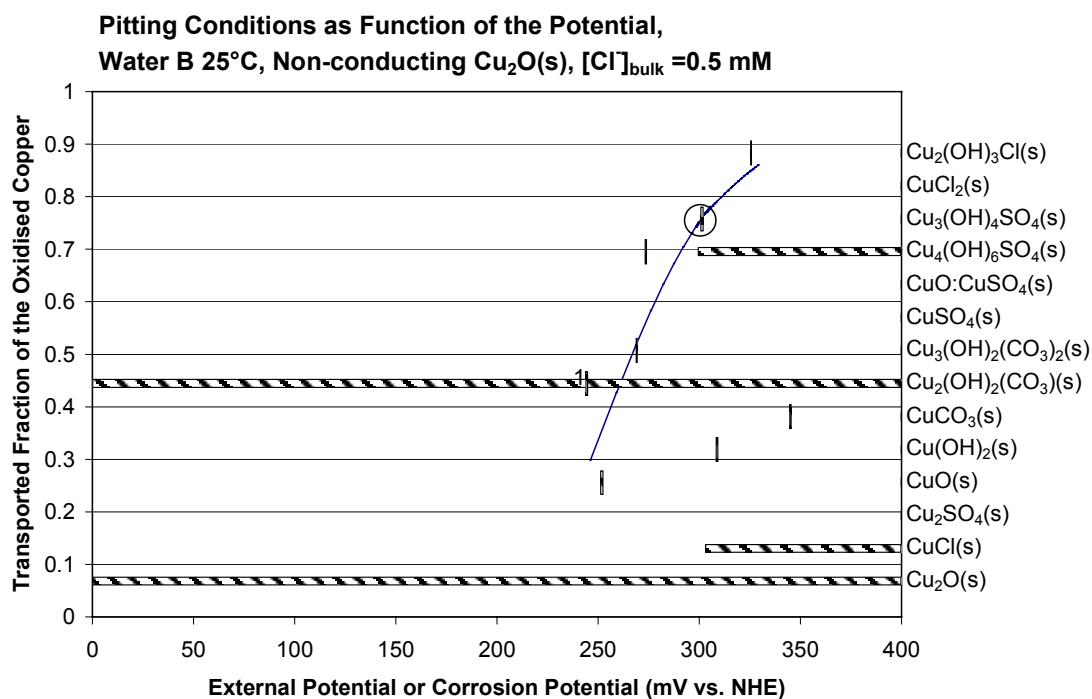


Figure 4-5. Diagram showing the distribution of the corrosion products into a solid fraction and a dissolved fraction at the bottom of a corrosion pit. The curve shows the fraction of the oxidised copper which is formed as dissolved species, as function of the potential in the bulk solution outside the cavity. The horizontal bars in figure 4-labelled to the right of the diagram, indicate the composition of the solid corrosion products that form inside and outside the cavity. The vertical bars indicate coexistence potentials for $\text{Cu}_2\text{O}(\text{s})$ with the various cupric solids in a solution with pH and salt contents of the undisturbed bulk water outside the cavity. The ring indicates the point representing the pit illustrated in figures 4-1 to 4-4.

Table 4-2. Calculation of the excess fraction of copper for the products Cu₂O(s) and CuCl(s), respectively.

	Cu(s)	Cu ₂ O(s)	CuCl(s)	Units
Molar Weight	63.546	143.09	99	g/mol
Density	8.92	6	4.14	g/cm ³
Molar volume	7.12	23.85	23.91	cm ³ /mol
	7.12	11.92	23.91	cm ³ /mol Cu
Volume contents	0.14	0.08	0.04	mol Cu/cm ³
Excess Fraction Cu		0.40	0.70	mole/mole

In water B at 25°C with a chloride concentration of 0.5 mM, the fraction of the oxidised copper which is formed as dissolved species and is transported away from the surface reaches the value of 0.4 at about 260 mV. This potential can be said to be a theoretical limit for immunity against pitting corrosion of copper in this water.

The horizontal bars in figure 4-5, labelled to the right of the diagram, indicate the composition of the solid corrosion products that form inside and outside the cavity. Although a corrosion pit would be unable to develop and propagate at potentials below about 260 mV, we can still calculate the equilibria and transport rates for such conditions. The lower horizontal bar indicates that cuprous oxide, Cu₂O(s), is formed at the metal surface at all potentials. Basic carbonate malachite, Cu₂(OH)₂CO₃(s), is also formed at all potentials. Since we assume a finite concentration of dissolved oxygen in the bulk water and chemical equilibrium, all cuprous species diffusing outwards are eventually oxidised to cupric species. This oxidation occurs at all potentials and cupric solids precipitate under all the conditions we have studied.

The precipitation of the solid cupric species takes place outside the cavity. This is a consequence of the decreased pH inside the cavity, which prevents precipitation. The production of cupric species from the oxidation by dissolved oxygen contributes to the tendency of cupric solids to form outside the cavity.

At a potential of about 300 mV, cuprous chloride, CuCl(s), and basic sulphate brochantite, Cu₄(OH)₆SO₄(s), begins to form along with the previous solids. That these two solids appear at the same potential is a coincidence particular to this water composition. CuCl(s) forms at the bottom of the cavity whereas the basic sulphate forms outside the cavity but inside the layer of malachite and at a slightly lower pH.

The vertical bars indicate coexistence potentials for $\text{Cu}_2\text{O}(\text{s})$ with the various cupric solids in a solution with pH and salt contents of the undisturbed bulk water outside the cavity. We describe the pitting corrosion of copper as a case of galvanic corrosion. Dissolved oxygen is electrochemically reduced on a conducting phase of $\text{Cu}_2\text{O}(\text{s})$. This oxide can behave as an efficient cathode only if the access of oxygen to the surface is not blocked. If the oxide is not stable against oxidation to solid cupric phases, this oxidation would not only consume cathodic current, which could otherwise drive the anodic dissolution in a corrosion pit, but the build up of thick layers of cupric phases would make the access of oxygen to the underlying cuprous oxide more difficult. The vertical bar representing $\text{Cu}_2(\text{OH})_2\text{CO}_3(\text{s})$ appears at the lowest potential in figure 4- indicating that malachite is the most stable cupric phase in the bulk water. Because of the consumption of anodic current and because of the limited access of oxygen to an underlying layer of conducting $\text{Cu}_2\text{O}(\text{s})$, copper is unlikely to attain much higher corrosion potentials than this coexistence value. To the extent that higher corrosion potentials are attained the corrosion potential would be easily polarised and shifted to lower values by a demand of anodic current from a corrosion pit.

The highest potential at which $\text{Cu}_2\text{O}(\text{s})$ at an external surface is stable against oxidation to malachite is about 250 mV and the minimum potential for pitting corrosion is about 260 mV. We conclude that this water would favour general corrosion and not pitting corrosion.

Figure 4-6 shows the same data as figure 4-5 but for a water where the bulk chloride concentration has been increased to 0.5 to 4.0 millimoles per litre. The curve illustrating the fraction of the oxidised copper that forms aqueous species at the site of oxidation now shows a distinct peak at a potential of about 240 mV. The location of this peak coincides with the formation of $\text{CuCl}(\text{s})$ indicated in the figure 4-by the horizontal bar. The formation of $\text{CuCl}(\text{s})$ is the cause of the decrease in the fraction forming aqueous species. Because of the increased chloride concentration in the bulk water outside the cavity the formation of $\text{CuCl}(\text{s})$ starts at a lower potential than in figure 4-5 and larger fractions of the oxidised copper can precipitate as $\text{CuCl}(\text{s})$ because of the lower influence of concentration polarisation with respect to chloride ions.

At potentials higher than about 260 mV the curve representing the fraction of the oxidised copper forming aqueous species increases again. This increase is caused by the increasing influence of the electrochemical oxidation of copper metal to cupric species. Using the value of 0.4 for the fraction of the oxidised copper forming dissolved species at the site of the oxidation as a limit for pitting corrosion, we find that the potential would have to exceed about 270 mV for a corrosion pit to propagate in this water.

Conditions at a surface some distance from the cavity is not changed by the increased chloride concentration. The coexistence potential for $\text{Cu}_2\text{O}(\text{s})$ with atacamite, $\text{Cu}_2(\text{OH})_3\text{Cl}(\text{s})$ is shifted to a lower value but malachite is still the most stable cupric solid. The coexistence potential for malachite is unchanged and equal to about 250 mV. Since $\text{Cu}_2\text{O}(\text{s})$ at an external surface is not stable against oxidation to malachite at the potential of 270 mV, which was found to be the minimum value required for pitting corrosion, general corrosion would be favoured also in this case.

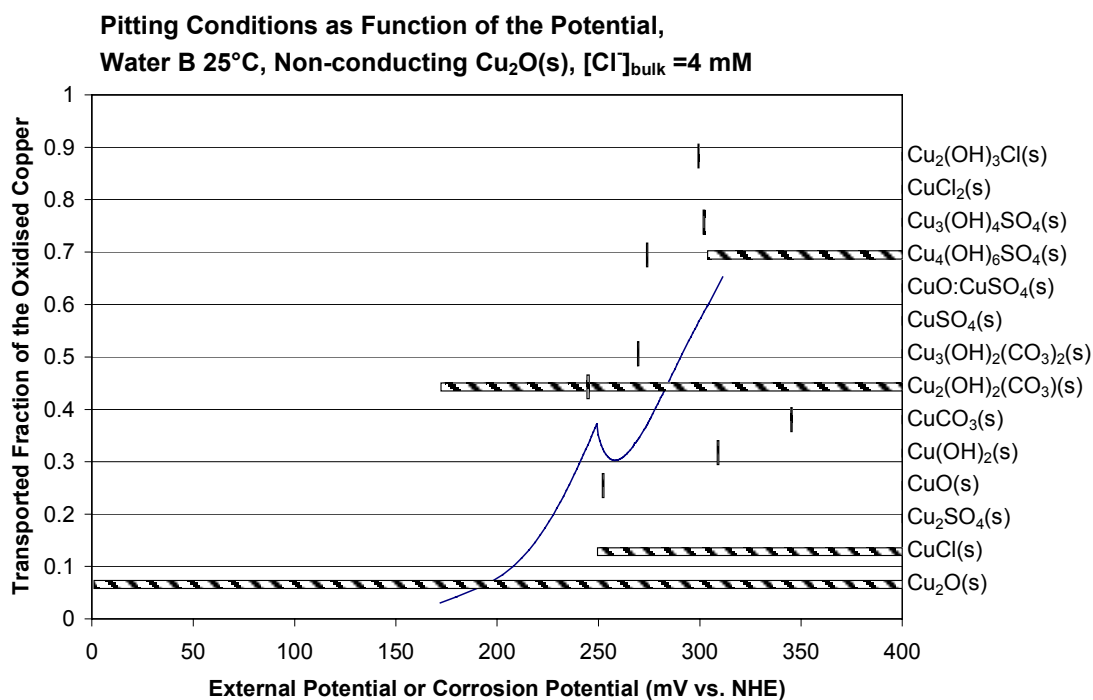


Figure 4-6. A diagram showing the distribution of the corrosion products into a solid fraction and a dissolved fraction at the bottom of a corrosion pit.

Figure 4-7 shows the same data as figures 4-5 and 4-6 but for a water where the bulk chloride concentration has been increased to 256 millimoles per litre. The drop in the curve is very sharp when the potential is reached where CuCl(s) can begin to form. At slightly lower potentials then curve reaches a value close to unity. This indicates that almost all of the corroding copper at the bottom of the pit forms aqueous species and only a small fraction forms Cu₂O(s).

The stability of malachite and other species not containing chloride is only marginally influenced by the increased concentration. The small influence that can be detected is caused by the change in activity coefficients. The coexistence potential for Cu₂O(s) with malachite is approximately the same as in the waters with lower chloride concentrations whereas the stability of atacamite, Cu₂(OH)₃Cl(s) has increased and the coexistence potential for Cu₂O(s) with this solid is about the same as the coexistence potential for Cu₂O(s) with malachite. The whole curve indicating the fraction of the oxidised copper, which is formed as dissolved species, is located at potentials where Cu₂O(s) is stable against oxidation to malachite or to atacamite. Cu₂O(s) at an external surface can therefore behave as a cathode for oxygen reduction and drive the anodic processes in a nearby corrosion pit without electrochemical corrosion of the cathode material itself.

A process that may interfere with this pitting mechanism is the chemical dissolution of Cu₂O(s) to aqueous chloride cuprous complexes. The renewal of the oxide layer consumes cathodic current, which could otherwise drive the anodic dissolution of copper metal in a corrosion pit. Moreover, oxidation of aqueous cuprous species by dissolved oxygen may also lead to precipitation of malachite or atacamite on top of the

$\text{Cu}_2\text{O}(\text{s})$. If there is a layer with poorly conducting $\text{Cu}_2\text{O}(\text{s})$, the solid cupric phases are insensitive to the reducing tendency of the low corrosion potential.

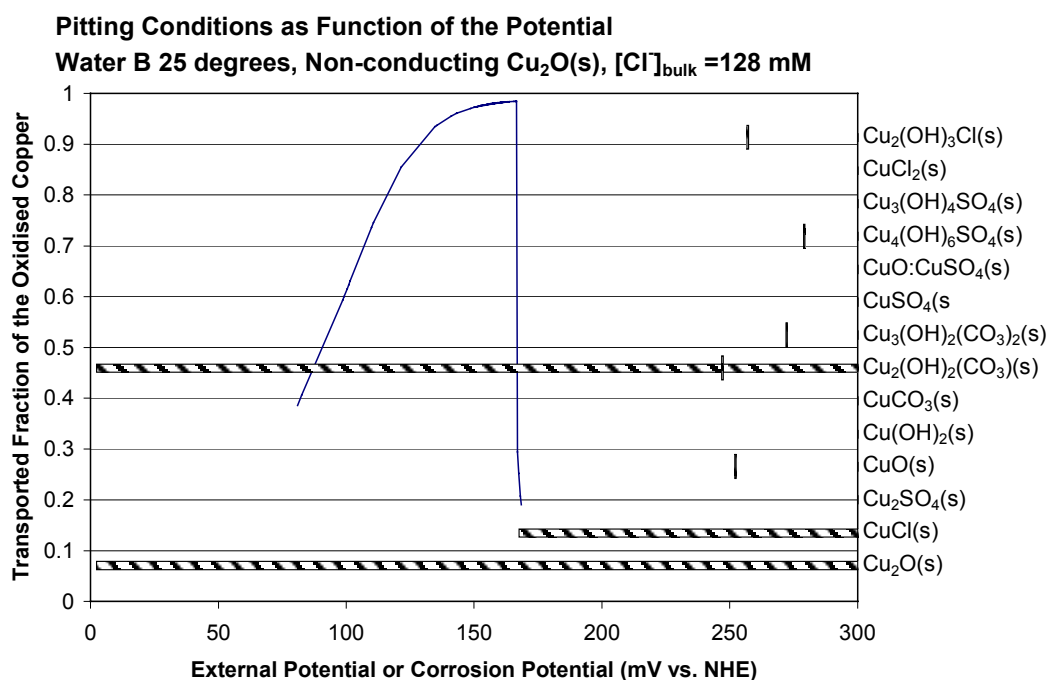


Figure 4-7. A diagram showing the distribution of the corrosion products into a solid fraction and a dissolved fraction at the bottom of a corrosion pit.

The curve indicating the fraction of the oxidised copper which is formed as dissolved species starts at about 0.4 in figure 4-7. In this water we find that already at the pH of the bulk, pH 7.0, $\text{Cu}_2\text{O}(\text{s})$ is so soluble that almost 40% of the oxidised copper forms oxide. This is discussed further in section 5.

More diagrams of the type shown in this section are shown in appendix 1.

4.1.2 The influence of the chloride concentration

Figure 4-8 shows a collection of curves indicating the fraction of the oxidised copper that is transported as aqueous species, for waters with varying chloride concentration. In waters where the chloride concentration is higher than 0.016 moles per litre the value drops sharply to low values. For clarity, only the rising parts of the curves for the waters with high chloride concentrations are shown.

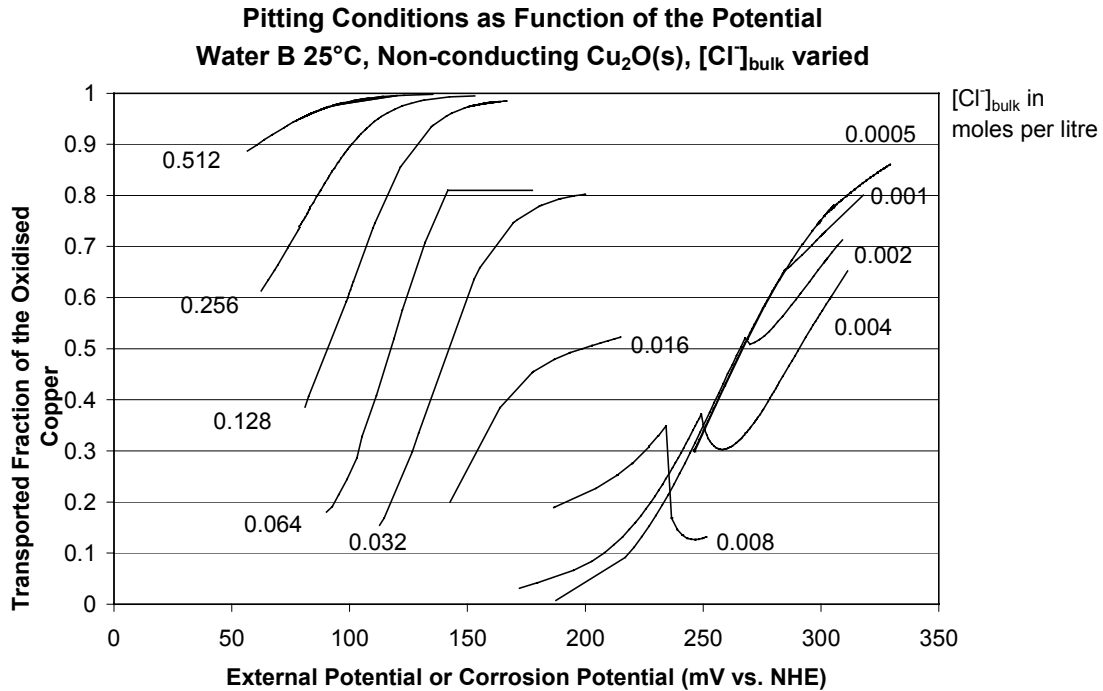


Figure 4-8. Curves showing the fraction of the oxidised copper which is formed as dissolved species, as function of the potential in the bulk solution outside the cavity. The chloride concentration in the bulk, belonging to each line is indicated in the figure. pH= 7.0 , total sulphate in the bulk=0.004 M and total carbonate in the bulk =0.0012 M.

If we collect the results for waters with varying chloride concentration we can draw a map over regions where we find pitting to be possible. Figure 4-9 shows such a map for 25 °C at pH 7.0.

The molar volume of copper in its solid oxides and salts is much higher than in copper metal. A continuing anodic dissolution at the front of a corrosion pit requires the presence of an aqueous electrolyte. Generally, this anodic dissolution results in a distribution of products into solids and dissolved species. We find that a large fraction of the oxidised copper will have to form aqueous corrosion products for propagation to be possible. If the fraction of the oxidised copper that forms solid phases i.e. Cu₂O(s), at the corroding copper surface is too high, the necessary aqueous transport of mass and charge would be obstructed and the pitting process would cease.

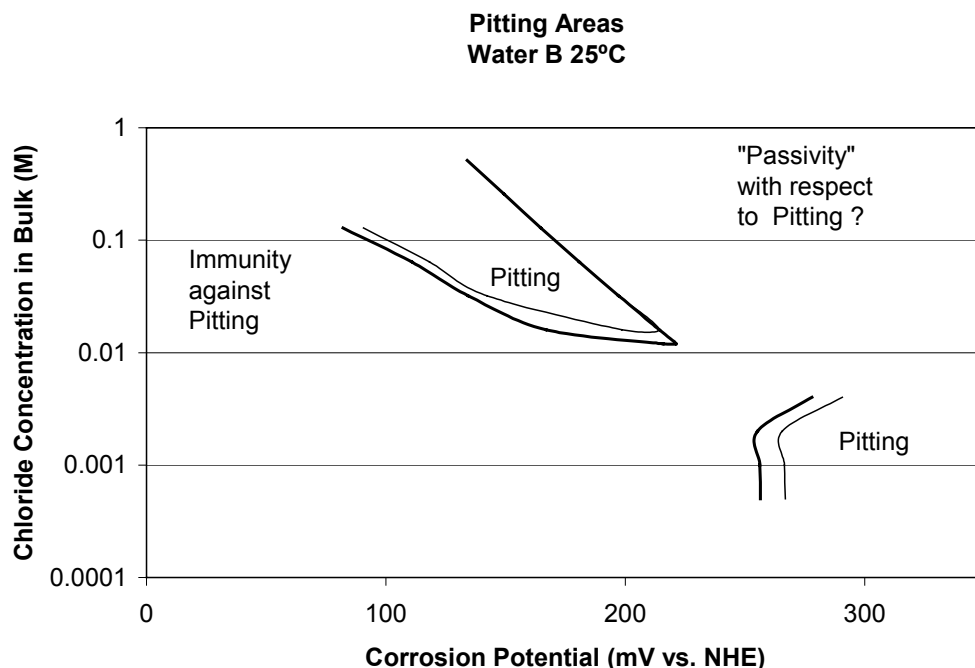


Figure 4-9. Potential – chloride concentration diagram with areas where we find that a corrosion pit can propagate. The thick line indicates that the fraction of the oxidised copper which transported away from the site of the oxidation as aqueous species is equal to 0.4, the thin line indicates conditions corresponding to the transported fraction equal to 0.5.

The formation of aqueous cuprous and cupric species is limited by the oxidation potentials for $\text{Cu(s)}/\text{Cu}^+$ and for $\text{Cu(s)}/\text{Cu}^{2+}$. At a given potential only a certain concentration, or rather activity, of Cu^+ and Cu^{2+} can be formed. The total concentration of Cu(I) and Cu(II) is determined by the degree of complex formation with anions such as hydroxide, chloride, sulphate and carbonate. At the same time these anions form solids with Cu(I) and Cu(II) and precipitation of these solids may limit the solubility and thereby also limit the total concentration of copper in solution.

During steady state, the distribution of the corrosion products into a solid fraction and an aqueous fraction is influenced also by the rates of transport. If we for simplicity consider only cuprous species, $\text{Cu}_2\text{O(s)}$ and aqueous Cu^+ are formed in proportions corresponding to the relative transport rates of H^+ , resulting from the oxide formation, and Cu^+ . Just as Cu^+ can be transported as chloride complexes CuCl(aq) , CuCl_2^- , etcetera, H^+ can be transported as $\text{H}_2\text{CO}_3(\text{aq})$. The transport as complex species requires of course a corresponding supply of chloride and hydrogen carbonate, respectively.

At low potentials where the influence of Cu^{2+} is small, we find that pitting is possible only in waters rich in chloride. However, if the potential is higher than a certain value in a chloride rich water, the solid CuCl(s) would begin to precipitate. Precipitation would take place immediately at the surface and the volume of the salt may take up a larger volume than the oxidised copper did in its metal form. This would lead to a pit overflowing with CuCl(s) . If propagation is at all possible under such conditions, it would be a low growth rate, because of the small aqueous cross section available for the necessary aqueous mass transport in any remaining channels in the salt. The modes of transport for such a pit would have to include mechanical extrusion of corrosion products. This is a mode of transport not considered in our model. Preliminarily we

regard this situation as a non-pitting state and we find that an upper potential limit for pitting may exist.

In waters with relatively low chloride concentrations, the transport of Cu^+ cannot compete with the rate of transport of H^+ . Pitting is then possible only at potentials where Cu^{2+} is formed in significant amounts. CuCl(s) may be formed also in such waters but the lower bulk concentration results in a lower fraction of the volume occupied by CuCl(s) and propagation by aqueous mass transport is still possible.

4.1.3 Influence of other water parameters

The roles of anions such as carbonate and sulphate are not the same in a low chloride water as in a high chloride water. To illustrate the influence of the concentrations of these and other components in the water we studied the effects in a low chloride water (0.5 mM) as well as in a water with medium high chloride concentration (32 mM).

4.1.4 The influence of the sulphate concentration

Figures 4-10 and 4-11 show the effect of the sulphate concentration of the bulk solution outside a corrosion pit on the distribution of the corrosion products into an aqueous fraction that is transported away from the surface and a solid fraction that remains at the site where it was formed. Figure 4-10 shows results for a low chloride water and figure 4-11 shows results for a medium high chloride concentration.

As shown in the figure 4-10 there is a relatively strong detrimental effect of increased sulphate concentrations in the low chloride water. Higher values of the transported fraction are obtained at a given potential when the sulphate concentration in bulk water outside the cavity is high.

In contrast, in the water with higher chloride concentration data points for the water with 8 millimoles sulphate per litre fall on the same curve as data for the water with 2 millimoles per litre. A significant change is seen only when the sulphate concentration is increased to the same level as the chloride concentration. When the sulphate concentration is increased to 32 millimoles per litre there is a beneficial effect of sulphate. Lower values of the transported fraction are obtained at a given potential when the sulphate concentration in bulk water outside the cavity is high.

Sulphate seems to have a detrimental influence with regards to pitting corrosion when the chloride concentration is low and a beneficial influence when the chloride concentration is high.

Analysis of the concentration profiles in and around the pits for the two cases reveals that in the low chloride water, the aqueous mass transport of copper is dominated by cupric species. At a given potential, the total equilibrium concentration of cupric species is increased by increased sulphate concentration. This leads to higher concentration gradients and higher rate of the aqueous mass transport for the aqueous corrosion products. In the water with higher chloride concentration, the aqueous mass transport of copper is dominated by cuprous species. Cupric species do not contribute because the redox potential is too low to produce significant amounts without aqueous oxygen. Although the iR drop is low in a water with high concentrations of salts, there is a tendency for negatively charged ions to enrich in the pit solution. When the

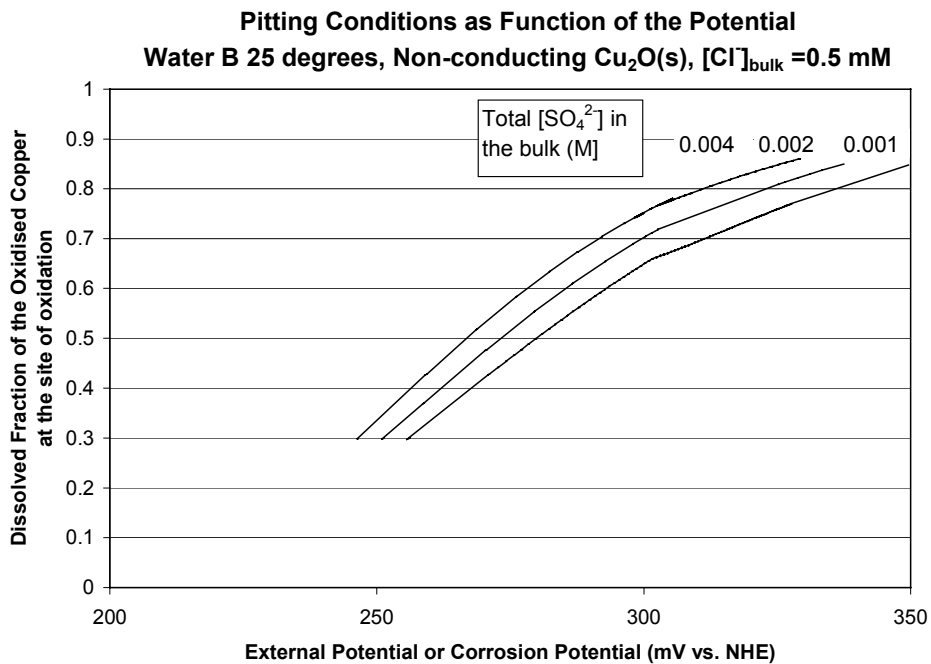


Figure 4-10. Curves showing the distribution of the corrosion products into a solid fraction and a dissolved fraction at the bottom of a corrosion pit. Variations in the bulk concentration of sulphate in a chloride poor water.

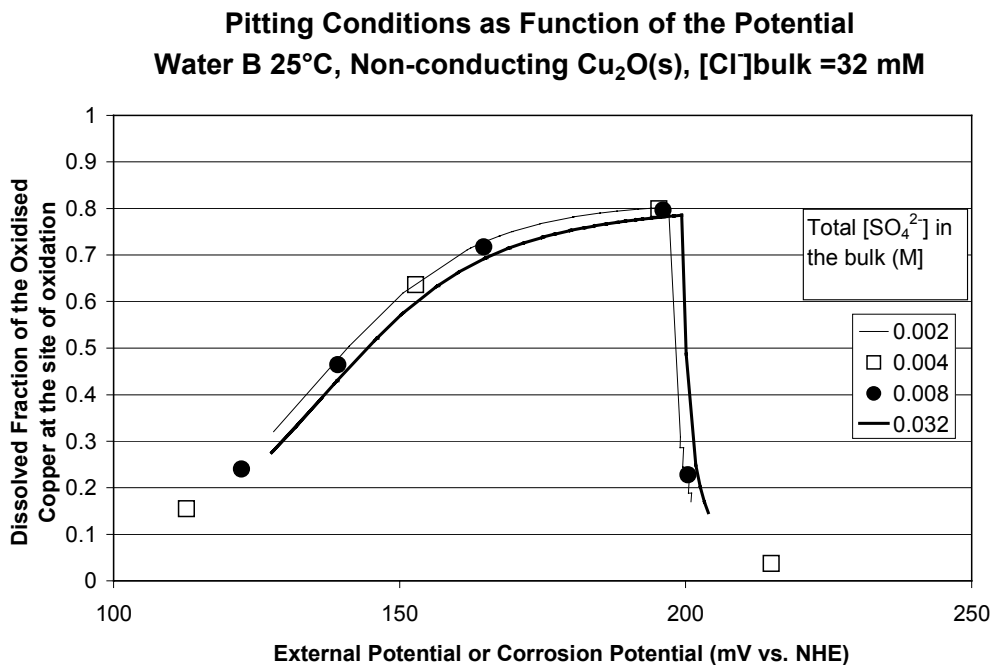


Figure 4-11. Curves showing the distribution of the corrosion products into a solid fraction and a dissolved fraction at the bottom of a corrosion pit. Variations in the bulk concentration of sulphate in a medium chloride rich water.

sulphate concentration is low, chloride is predominantly enriched. When the sulphate concentration is increased to the same level as the chloride concentration, sulphate is predominantly enriched because of its higher charge. At the same time the iR-drop decreases further because of the increased conductivity of the solution. The decrease in the enrichment of chloride ions in the pit solution that occurs when the sulphate concentration is increased, has the effect of decreasing the equilibrium concentration of cuprous species and thereby decreasing the fraction of the oxidised copper that is transported away from the site of oxidation.

4.1.5 The influence of the total carbonate concentration

Figures 4-12 and 4-13 show effects of the total carbonate concentration of the bulk solution outside a corrosion pit on the distribution of the corrosion products into an aqueous fraction that is transported away from the surface and a solid fraction that remains at the site where it was formed.

In the low chloride water in figure 4-12 data points for a water where the carbonate concentration was decreased by a factor of two fall practically on top of the curve for the water with higher carbonate concentration.

In the water with higher chloride concentration in figure 4-13 there is a systematic beneficial effect of increased carbonate concentrations. An increase in the carbonate concentration shifts the potential required to obtain a certain value of the transported fraction to higher values. Increased carbonate concentration do not interfere with the precipitation of CuCl(s) and the sharp drop in the curves occur at the same potential.

The potential window where the transported fraction is higher than the pitting limit, 0.4, becomes gradually more narrow as the carbonate concentration is increased.

4.1.6 The influence of the bulk pH

Figure 4-14 and 15 show effects of the pH of the bulk solution outside a corrosion pit on the distribution of the corrosion products into an aqueous fraction that is transported away from the surface and a solid fraction that remains at the site where it was formed.

As the figures show the curves are practically independent of the bulk pH in the low chloride water as well as in the water with higher chloride concentration. The bulk pH seems to have little influence on the pitting potential.

4.1.7 The influence of the concentration of dissolved oxygen

Figure 4-16 and 17 show effects of the oxygen concentration in the bulk solution outside a corrosion pit on the distribution of the corrosion products into an aqueous fraction that is transported away from the surface and a solid fraction that remains at the site where it was formed.

As the figures show there is a small beneficial effect of increasing oxygen concentration in the bulk water. A high oxygen concentration requires higher potentials to cause pitting corrosion. The cause for this beneficial influence of dissolved oxygen can be seen in figures A-20 and A-21. In the third figure 4-in A-21 showing the transported fraction of the dissolved copper as function of the local pH,

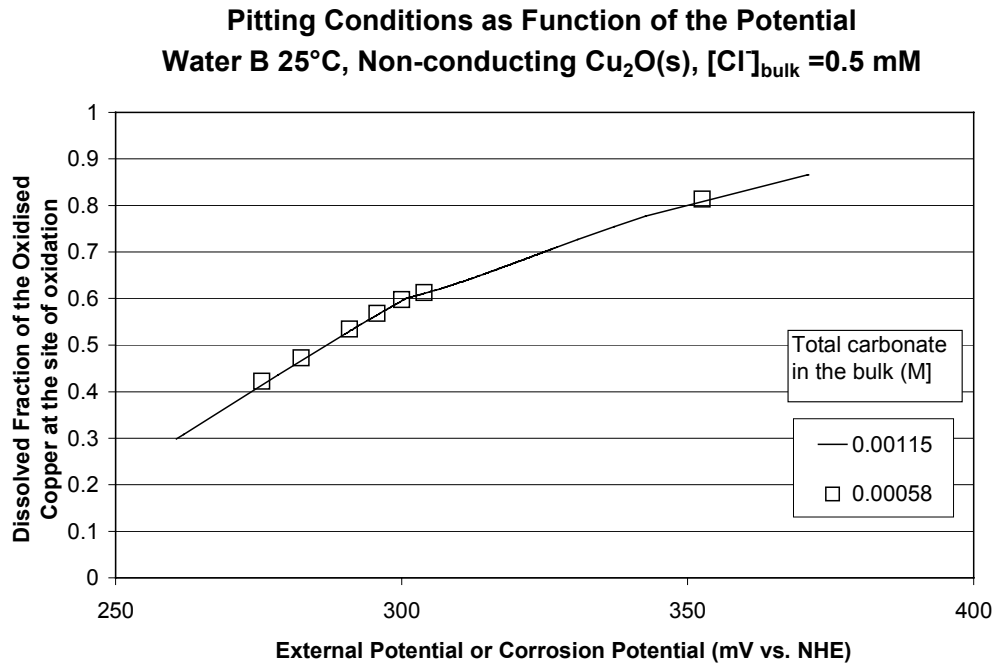


Figure 4-12. Curves showing the distribution of the corrosion products into a solid fraction and a dissolved fraction at the bottom of a corrosion pit. Variations in the bulk total concentration of carbonate in a low chloride water.

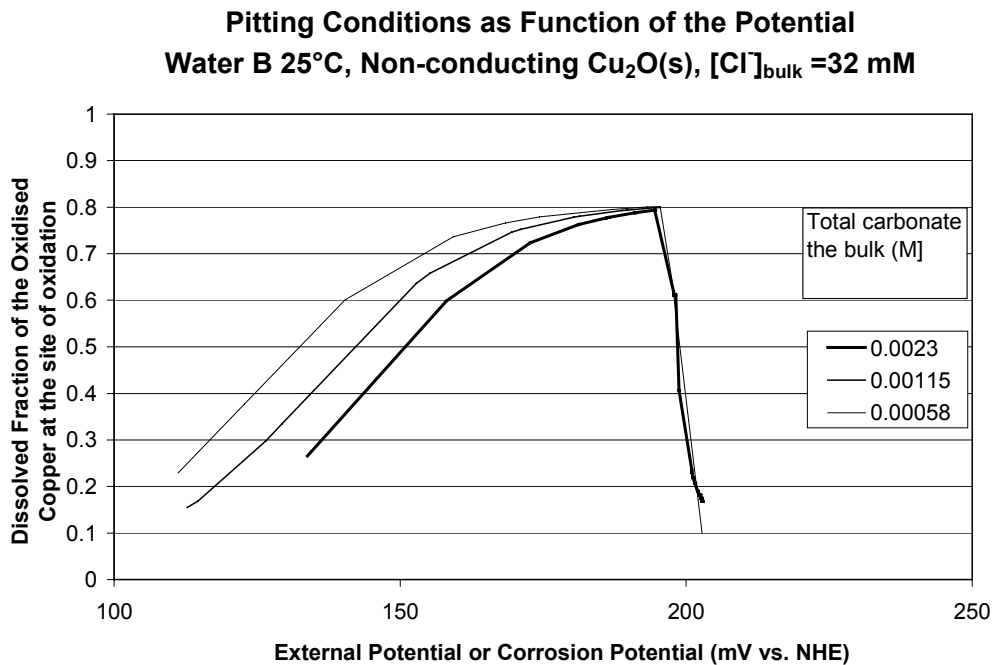


Figure 4-13. Curves showing the distribution of the corrosion products into a solid fraction and a dissolved fraction at the bottom of a corrosion pit. Variations in the bulk total concentration of carbonate in a medium chloride rich water.

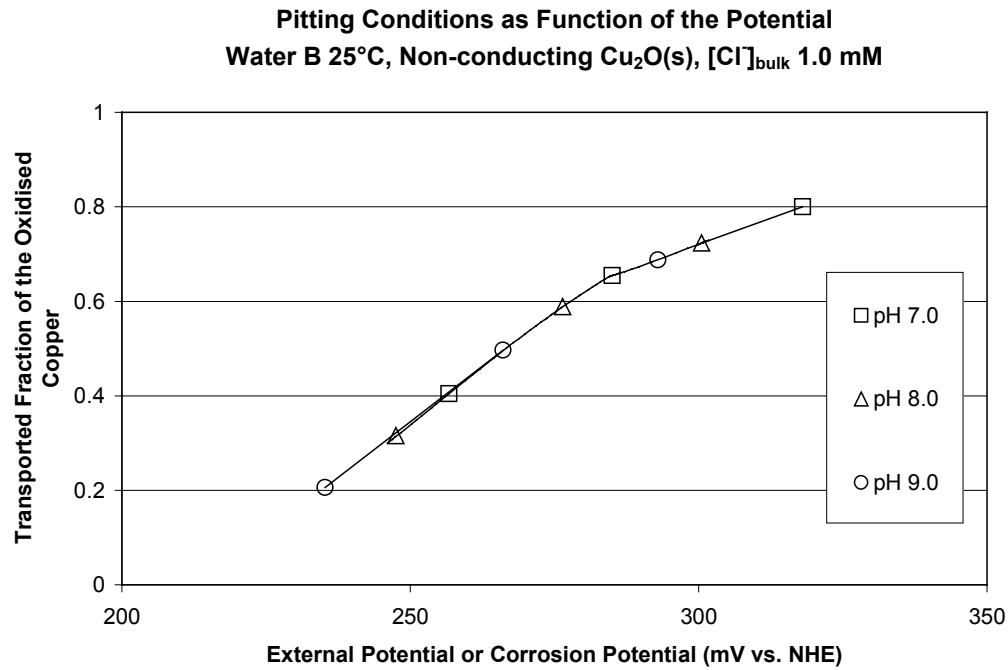


Figure 4-14. Curves showing the distribution of the corrosion products into a solid fraction and a dissolved fraction at the bottom of a corrosion pit. Variations in the bulk pH of a low chloride water.

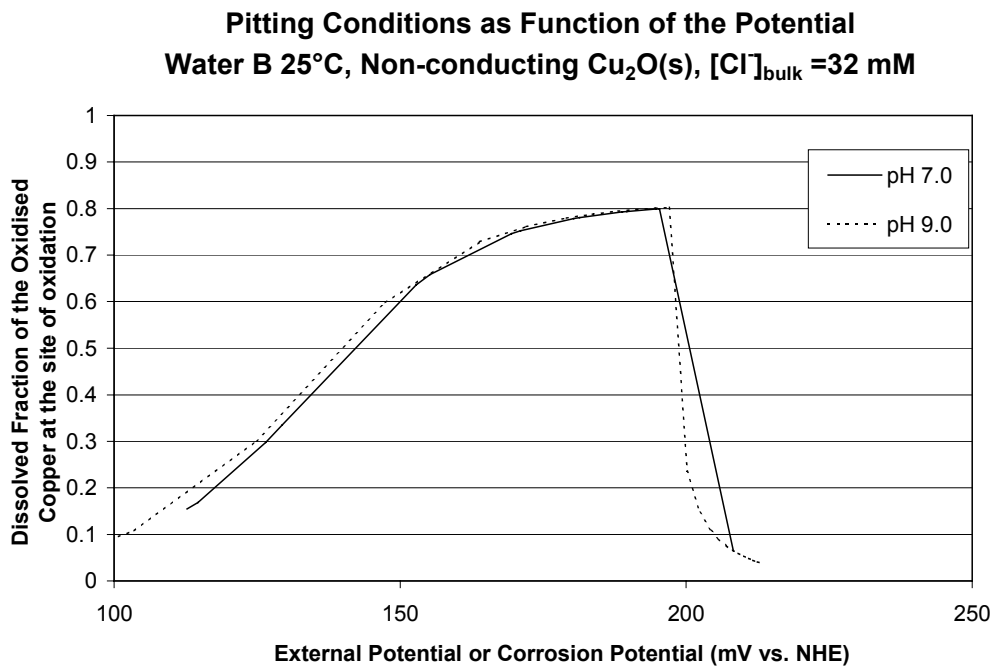


Figure 4-15. Curves showing the distribution of the corrosion products into a solid fraction and a dissolved fraction at the bottom of a corrosion pit. Variations in the bulk pH of a medium chloride rich water.

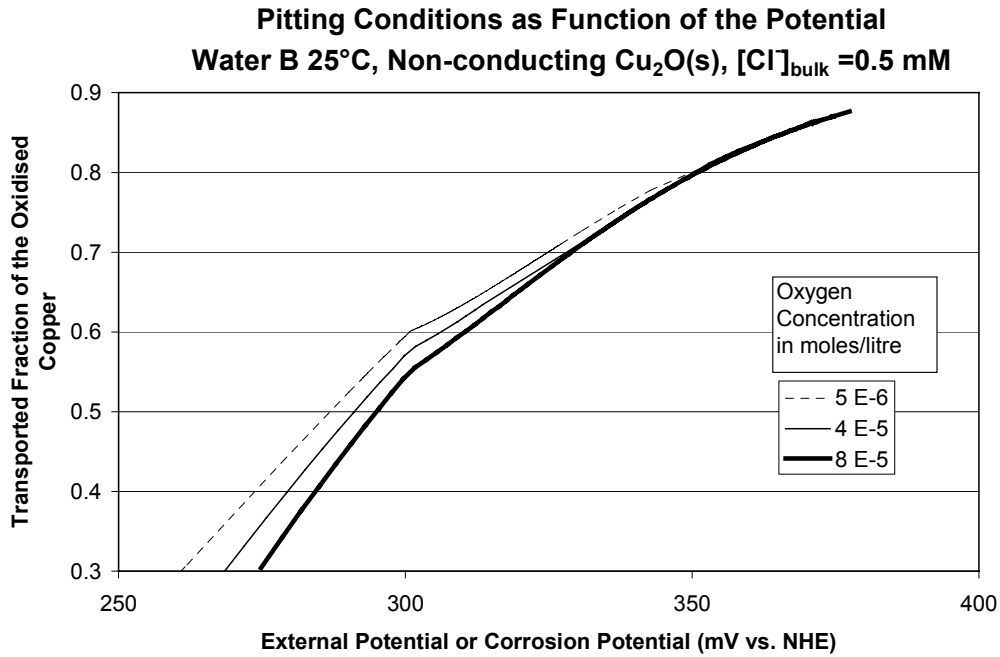


Figure 4-16. Curves showing the distribution of the corrosion products into a solid fraction and a dissolved fraction at the bottom of a corrosion pit. Variations in the bulk oxygen concentration in a chloride poor water.

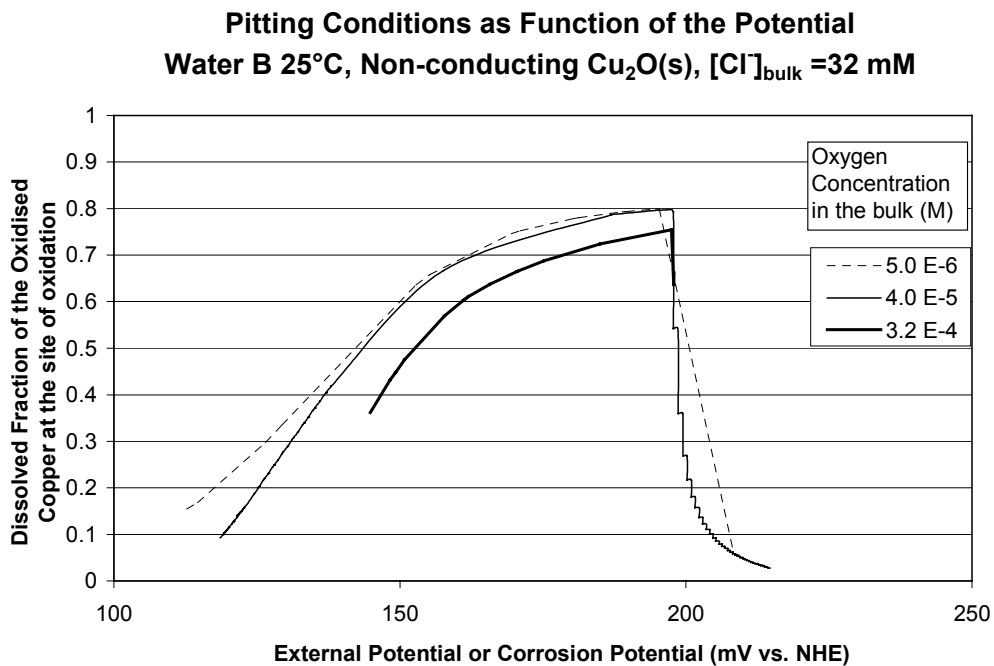


Figure 4-17. Curves showing the distribution of the corrosion products into a solid fraction and a dissolved fraction at the bottom of a corrosion pit. Variations in the bulk oxygen concentration in a medium chloride rich water.

the aqueous transport of cupric species appears with negative sign at low pH-values. The homogeneous oxidation of cuprous species to cupric at about pH 5.7 results in a high concentration of cupric species at that pH. The relatively low corrosion potential ensures that the concentration of cupric species at the corroding metal surface is low. Consequently, cupric species produced through homogeneous oxidation by dissolved oxygen, diffuse inwards and are reduced electrochemically to cuprous species at the metal surface.

4.1.8 Pitting corrosion at 75°C

In figure 4-18 we have assembled curves describing the transported fraction of the oxidised copper as function of the corrosion potential or external potential.

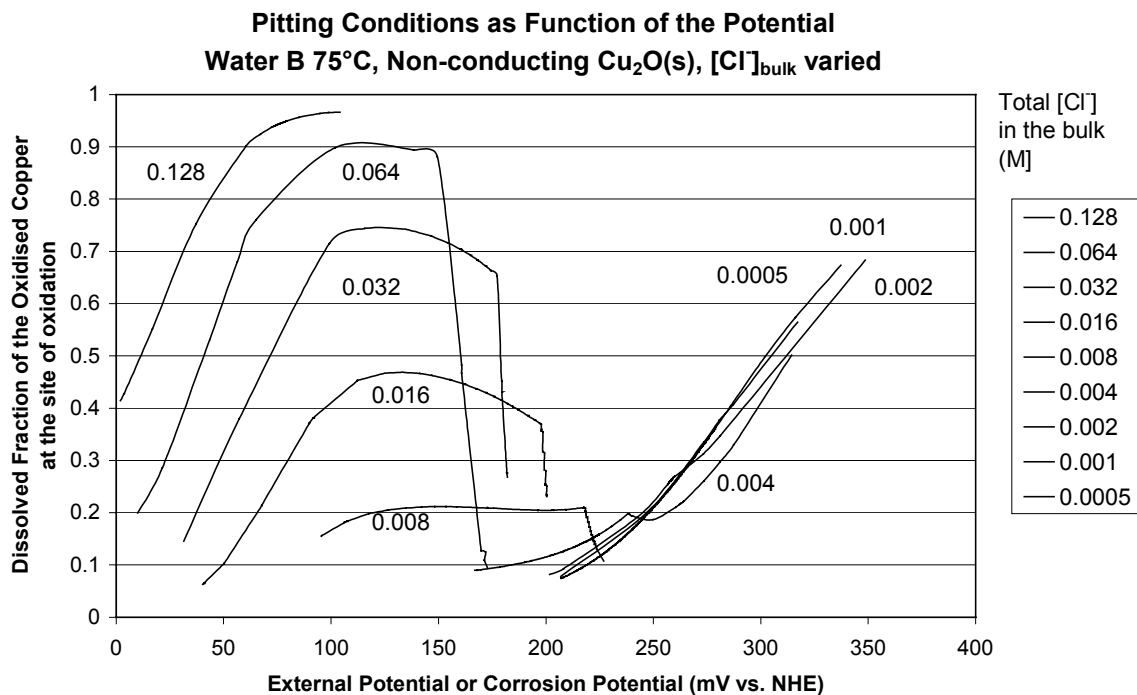


Figure 4-18. Curves showing the fraction of the oxidised copper which is formed as dissolved species, as function of the potential in the bulk solution outside the cavity. The chloride concentration in the bulk, belonging to each line is indicated in the figure. pH= 7.0 , total sulphate in the bulk=0.004 M and total carbonate in the bulk =0.0012 M.

The trends are same as shown in figure 4-8 for 25°C. Pitting corrosion seems to be possible at low chloride concentrations and at high chloride concentrations. At concentrations of about 10 milli moles chloride per litre there is no potential range where we can find propagating pits consistent with the assumptions. In contrast to the results obtained for 25°C, we here, for the medium chloride rich waters, find maxima in the curves before the potential where CuCl(s) starts to form.

4.2 The existence of multiple solutions

In the calculations, we use the fluxes of components, to and from the undisturbed bulk water, to control the formation of aqueous and solid corrosion products. In many cases

we find that there are several combinations of fluxes from the bulk which lead to corrosion pits which seem to be consistent with the assumptions. This multiplicity of states is found mainly when the oxygen flux is varied. As a consequence of a varied oxygen flux, the location of precipitated solids, in terms of pH, and the distribution of the corrosion products between the various solid and aqueous species change. We have tried to be consistent and use the lowest possible oxygen flux that leads to propagating pits according to the assumptions. The argument behind that choice is that the use of higher oxygen fluxes leads to net dissolution of $\text{Cu}_2\text{O}(\text{s})$ from some elements. In a finite element method net dissolution from an element would not be consistent with the assumption of stationary propagation. However, in our model the elements have neither fixed size nor fixed location. Net dissolution can be allowed in the inner parts of the modelled corrosion pit because the location of the element is shifted inwards, to a location where $\text{Cu}_2\text{O}(\text{s})$ previously has precipitated, as the pit grows. This shift inwards causes an implicit supply of $\text{Cu}_2\text{O}(\text{s})$ which can be allowed to dissolve. The same argument can not be used in the outer parts of the modelled pit. The model includes also outside the cavity. As the pit grows the location of the outer elements, where solids are present, are shifted outwards into a range where there previously was no solid so no net dissolution can be allowed.

In terms of the dissolved fraction of the oxidised copper at the innermost place in the cavity, as function of the potential, results seem to be insensitive to the multiplicity of states. Although the distribution between corrosion products may vary, the points representing the corrosion pits fall on the same line.




Diagrams A-26 to A-29 illustrate the effects of the multiple solutions. The solid line in diagram A-27 indicates results for an oxygen flux close to the minimum value. Diagram A-28 shows results for increasingly high oxygen fluxes. The curve in diagram A-28 is shown also in diagram A-26, dashed, for comparison. The two curves show only minor differences. The detailed diagrams illustrate the effect of an increased oxygen flux. Net dissolution of $\text{Cu}_2\text{O}(\text{s})$ is the consequence as illustrated by the increase in the transported fraction at pH 5.0 in the second diagram in A-29.

4.3 Error analysis

The sensitivity of the results to minor changes in input data was studied by changing the value of one parameter at the time. Stability constants for the cupric solids were not studied in this way. Variations in the pH of the bulk water leads to big changes in the distribution of the corrosion products into the various solids that precipitate. Nevertheless, Results from pH 7.0 falls on the same line as results from pH 9.0 as shown in figures 4-14 and 4-15. We conclude therefore that the results, in these terms, are relatively insensitive to minor variations in the values used for the stability constants for cupric solids. The parameters that were varied are shown in table 4-3.

The diagrams A2 and A17 show that variations in a single value of the magnitude indicated in table 4-3 cause minor differences in the results expressed as the transported fraction of the oxidised copper at the bottom of the pit as function of the potential. Meaningful results are obtained also when a considerable uncertainty in the input data is allowed for.

Table 4-3. Parameters varied in the error analysis

Error analysis			Symbol
<i>lg k</i> for Cu ₂ O(s) increased	0.1	units to 0.8445	
<i>lg k</i> for CuCl ₂ ⁻ increased	0.3	units to 5.988	+
<i>lg k</i> for CuSO ₄ (aq) increased	0.3	units to 2.611	
<i>D</i> for all aqueous cuprous species increased by a factor of 2			

The symbols in table 4-3 refer to the diagrams A2 and A17 in appendix 1.

5 Corrosion of copper in chloride rich waters

In chloride rich waters we find that cuprous oxide is very soluble. At concentrations above about 0.1 M we cannot find the lower potential limit for immunity against pitting corrosion. The reason is that already at neutral to slightly alkaline pH-values $\text{Cu}_2\text{O}(\text{s})$ may be too soluble to form a protective layer on the underlying copper metal. Figure 5-1 shows the equilibrium concentrations of aqueous $\text{Cu}(\text{I})$ as function of the chloride concentration for pH 7, 8 and 9.

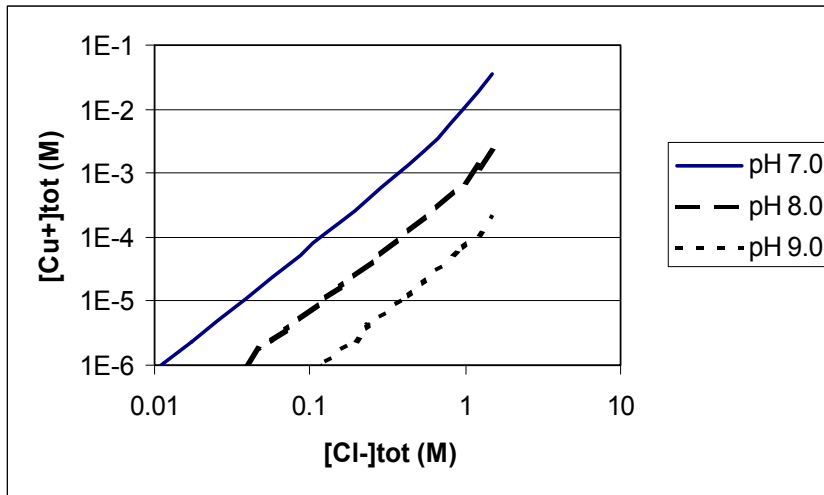


Figure 5-1. Total concentration of dissolved cuprous copper in equilibrium with $\text{Cu}_2\text{O}(\text{s})$ as function of the chloride concentration at pH 7.0, 8.0 or 9.0.

In these chloride rich waters, corrosion can proceed without the local acidification caused by formation of $\text{Cu}_2\text{O}(\text{s})$. We find no reason why this corrosion would take the form of localised corrosion, indeed many phenomena would seem to favour even, general corrosion and not localised corrosion.

However, it is conceivable that at some sites the cuprous oxide is protected from dissolution by adherent cupric phases or other solids. At places between such protected sites the corrosion may proceed and have the appearance of localised corrosion. A site under this mode of corrosion is illustrated in figure 5-2.

The layer of cuprous oxide, which is not protected from dissolution, may be very thin or even absent. The main difference between this mode of corrosion and the pitting corrosion described in section 4 is that under pitting corrosion there is a local environment with decreased pH. The decrease in pH is caused primarily by net formation of $\text{Cu}_2\text{O}(\text{s})$, although not sufficient to protect the underlying copper metal. In the type of corrosion we are describing here, no local acidification is necessary. Acidification is limited to the higher pH-ranges where cupric solids are formed, because there is no net production of $\text{Cu}_2\text{O}(\text{s})$.

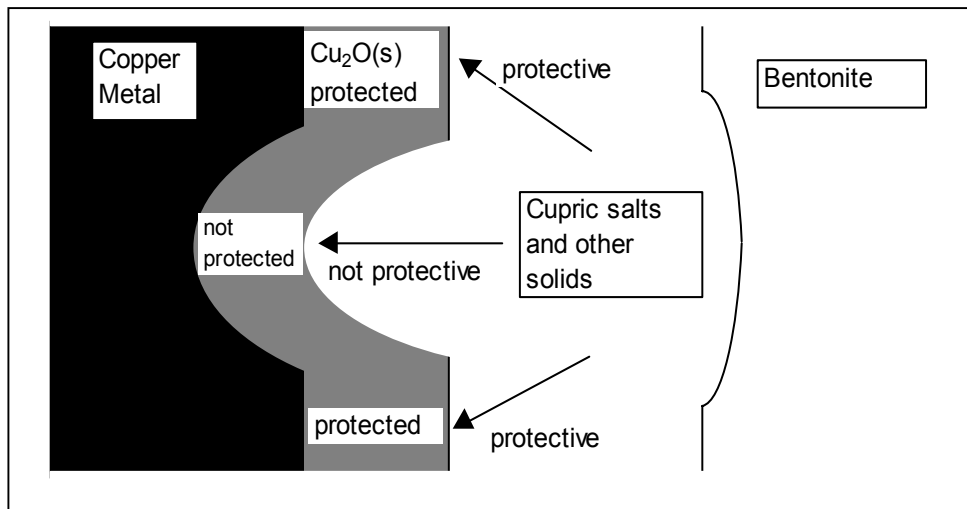


Figure 5-2. Schematic illustration of a site under general corrosion. Because of protection of adjacent sites the attack has the appearance of localised corrosion.

Significant aqueous mass transport of oxidised copper is here possible because of the high solubility of $\text{Cu}_2\text{O}(\text{s})$. When this flux of $\text{Cu}(\text{I})$ encounters oxygen diffusing through bentonite solid cupric phases are formed. Depending of the exact composition of the water in terms of content of carbonate and chloride and pH, malachite, atacamite or tenorite may form. These phases have rather low solubilities.

Probable reactions are:



The production of voluminous corrosion products is possible only if the bentonite yields to the pressure exerted by the corrosion products. This is illustrated in figure 5-2 by the curved boundary between corrosion products and bentonite

If this scenario cannot be disproved then we may also have to take the next step. If $\text{Cu}_2\text{O}(\text{s})$ can be protected from dissolution by cupric phases at places outside the cavity then the same may be true for surfaces in the cavity. That is, sites where $\text{Cu}_2\text{O}(\text{s})$ has been under dissolution can become protected by cupric phases which are forced towards the dissolving surface by the volume expansion caused by precipitation of cupric phases at the site where $\text{Cu}(\text{I})$ diffusing outwards encounters oxygen diffusing inwards. This step is illustrated in figure 5-3.

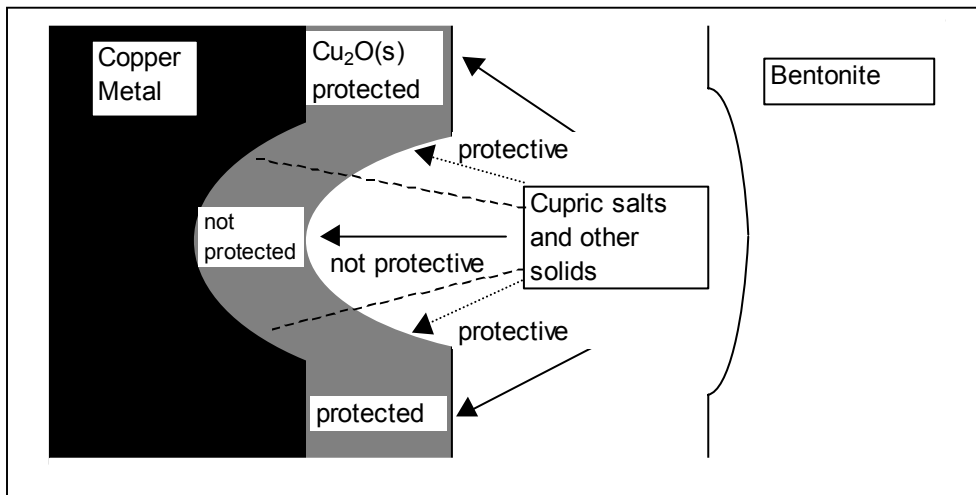


Figure 5-3. Schematic illustration of a site under general corrosion. Because of protection of adjacent sites the attack has the appearance of localised corrosion. Previously dissolving sites are becoming protected by cupric phases.

Figure 5.4 illustrates how such a corrosion attack can develop and grow preferentially deeper and not wider so that an essentially cylindrical cavity is formed.

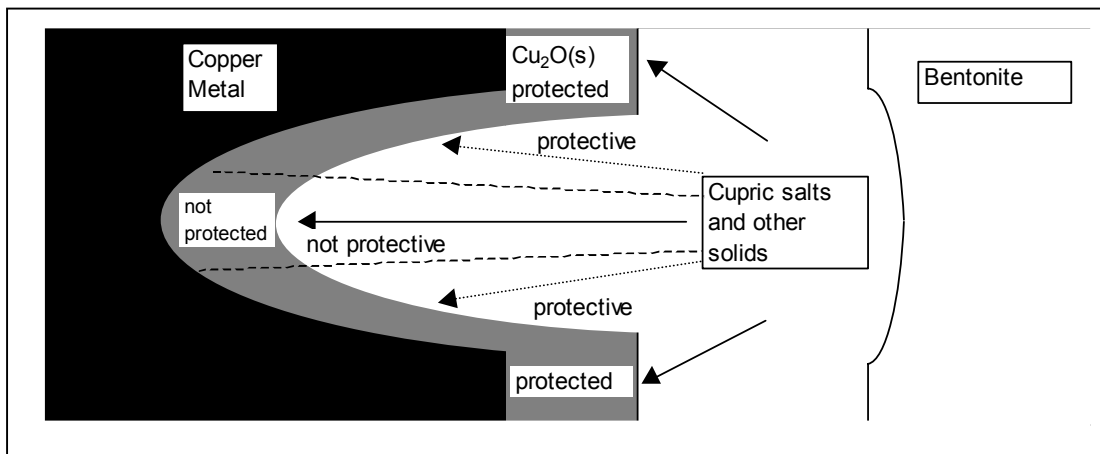


Figure 5-4. Development of a local corrosion attack by a process similar to general corrosion but where large fractions of the surface are protected from dissolution by cupric phases. Previously dissolving sites are becoming protected so that the cavity grows preferentially deeper and not wider.

In the previous discussion it has been implicitly assumed that somewhere at the canister surface there is a site where there is an electrochemical reduction of an oxidising agent

so that the local electrochemical oxidation of copper metal to cuprous species can be sustained.

The oxidation of the cuprous species to cupric species, mainly solids, takes place via homogeneous oxidation by dissolved oxygen. This oxidation takes place where the two concentration profiles meet and results in a very low concentration of Cu(I). The exact location of this place where dissolved cuprous species are oxidised to solid cupric phases is determined by the relative concentrations and diffusion rates of dissolved oxygen diffusing inwards through the bentonite and cuprous species diffusing outwards from the dissolving cuprous oxide. High concentration of oxygen outside the bentonite has the effect of shifting the location close to the cavity or even into the cavity. High concentrations of Cu(I) arising from high chloride concentration or low pH has the effect of shifting the location away from the cavity, even into the bentonite.

The volume expansion caused by the production of solid cupric phases results in a pressure high enough to physically move bentonite and previously existing corrosion products. Considering the mechanical properties of wet clay, which will yield to pressure but slowly, it seems reasonable that higher pressures and higher forces will arise closer to the site of solid formation than further away. The higher mechanical forces closer to the opening of the cavity than deep into the cavity may be invoked as an argument for why there should be better protection of Cu₂O(s), against dissolution, closer to the opening than deeper into the cavity. The argument can be formulated so that higher forces between the two phases results in better coverage and fewer sites where cuprous oxide is exposed to the chloride rich water. Within the limits of this argument we can say that there is a mechanism favouring cylindrically shaped cavities growing preferentially deeper and not wider rather than cavities with hemispherical shape.

6 Discussion

6.1 Copper and water

Copper metal is not stable in water containing dissolved molecular oxygen. Normally, the underlying copper metal is more or less protected by its corrosion products, mainly by cuprous oxide, $\text{Cu}_2\text{O}(\text{s})$.

Pitting corrosion occurs when the corrosion products locally fail to give sufficient protection of the metal against an aqueous electrolyte. A local corrosion attack may appear at a site where the formation of the corrosion products themselves creates a more aggressive electrolyte than the bulk solution. This is the case for what is normally termed pitting corrosion. However, a corrosion attack, which in all aspects has the same consequences as pitting corrosion, may occur when large parts of a construction in an aggressive bulk solution is somehow protected by deposited solids. A small part of the surface may not be thus protected and therefore exposed to the aggressive bulk solution. This is a mode of localised corrosion that seems particularly important in soil systems with high chloride contents.

Copper is not much used in seawater. Without alloying with other elements such as aluminium, copper is not sufficiently corrosion resistant in this environment. The morphology of the corrosion attacks is described as strong uneven general corrosion.

It does not seem unreasonable that substances from soil or bentonite clay pressed against the copper surface may provide a protecting barrier between the copper surface and the aggressive solution. Likewise, it does not seem unreasonable that this protection is imperfect at some sites. Depending on the area ratio between protected and not protected sites the corrosion will take the form of localised corrosion or of general corrosion.

6.2 Solid corrosion products on copper

Figure 6.1 shows schematically the layers of corrosion products that may appear on a copper surface.

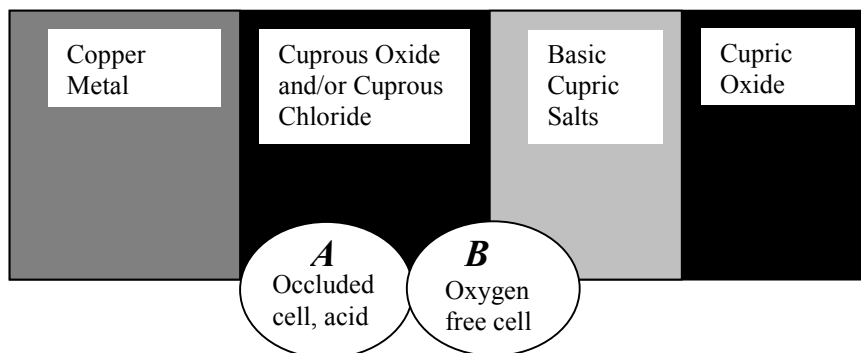


Figure 6.1 Schematic illustration of layers of corrosion products on copper with volumes of open solution. *A* corresponding to high solubility because of acidification and the build up of aggressive solution because of the corrosion process and *B* corresponding to high solubility because of a chloride rich bulk solution that gives high solubility to cuprous species and low solubility to cupric species.

For case *A*, the conditions for pitting used in section 4 are applicable. That is there is no pitting when further corrosion produces adherent and covering cuprous oxide. For case *B*, it will not matter how adherent and covering the cuprous oxide is formed at the copper metal surface. The cuprous oxide may dissolve from the outside because of the high solubility of cuprous copper in chloride rich water. In both cases it is assumed that there is porosity in the layers of cupric solids so that aqueous mass transport is possible. Either one of the solid cupric phases in figure 6-1 may be non-existent.

6.3 Extrusion of corrosion products

In the model for propagation of a corrosion pit we consider only aqueous mass transport. Extrusion of corrosion products through mechanical forces is neglected. Some requirements for such an extrusion are discussed here with emphasis on the possibility of extrusion of cuprous oxide formed at the bottom of the pit so that pitting may propagate.

We consider an existing corrosion pit where the corroding metal surface is almost covered by corrosion products. New corrosion leads to that a certain fraction of the corroded copper forms solid phases and the rest forms aqueous species. If the volume of the solids is larger than the volume of the corroded copper metal, then propagation is possible only if corrosion products outside this new formed corrosion products are shifted away from the surface and the old and the new corrosion products retains a porosity so that aqueous transport is possible.

At a grain in the porous corrosion products there are sites where there is contact with neighbouring grains and sites where the distance to the next grain is large. The physical movement of corrosion products requires that the grains of solid particles grow at sites where there is interference with neighbouring grains. These sites of growth must because of this interference be energetically less favourable than sites without interference.

The tendency of a grain or crystal to have an ordered lattice and to grow preferentially at sites favourable to the crystal can to various extents overcome the interference energy. Extrusion of corrosion products seems to be possible when the tendency of the grains to grow at sites favourable to the crystal dominates over the interference energy. High interference energy implies that the new atom to be added to a crystal will have to squeeze in into a restricted volume, energetically too close to atoms in a neighbouring grain. Mechanical energy is exerted when this energy is relaxed and has the effect of pushing the interfering grain away. This movement of a grain causes a chain reaction so that new unfavourable interference arises between grains and other grains also move. The more grains that have to move the higher the interference energy required to move them.

If a corrosion pit is filled with solid porous corrosion products, then all of the grains have to move. The deeper the pit the more solids have to move and higher energy is required to move them. Only a fraction of the dissolved corrosion products have the energy to attach to a grain at such an unfavourable site. Competing reactions are attachment to a grain at a site with less interference and the formation of a new grain.

Both of these competing reactions have the effect of decreasing the porosity and thereby decreasing the rate of propagation.

If extrusion of corrosion products from a corrosion pit caused by the extra volume required for the formation of a solid phase at the bottom of the pit is possible, then its importance will at least decrease with increasing pit depth.

7 Conclusions

- The main conclusions drawn in the previous phase of the work are not contradicted by the present results.
- The combined effect of potential and water composition on the possibility of pitting corrosion is more complex than was realised. The present results indicate that pitting corrosion can take place only over a certain potential range and that there is an upper potential limit for pitting as well as a lower.
- While increased sulphate concentrations aggravate a pitting situation continuously, results indicate the existence of a window in the chloride concentration where the minimum pitting potential increases sharply with increasing chloride concentration.
- Actually, results indicate the existence of a window in the chloride concentration where an increased sulphate concentration has a small beneficial influence. At a chloride concentration of about 32 mM, pitting is possible at potentials between about 140 mV and 200 mV (vs. NHE). The concentration in the pit is higher than 32 mM because of the potential gradient. An increased sulphate concentration decreases the potential gradient and thereby decreases also the chloride concentration in the pit and pitting requires slightly higher potentials.
- Represented in a $\lg [\text{Cl}]_{\text{tot}}$ – potential diagram, pitting ranges appear as two separate areas. At relatively low chloride concentrations, pitting is possible although saturation and precipitation of CuCl(s) takes place at the innermost sites in the cavity. At higher chloride concentrations, large amounts of CuCl(s) would precipitate. So large that the volume increase of solids, in the cavity, is not consistent with continued growth of the pit. At even higher chloride concentrations, pitting is possible without the formation of CuCl(s) .
- At high chloride concentrations (>20 mM) there may exist an upper potential limit for pitting. Above this potential limit, propagation of the pit is prevented by excessive precipitation of large volumes of CuCl(s) .
- A sensitivity analysis indicates that the model gives meaningful predictions of the minimum pitting potential also when relatively large errors in the input parameters are allowed for.
- Strongly uneven corrosion seems possible also without formation of locally more aggressive solutions. Particularly in soil systems, parts of a copper surface may be protected from corrosion by solids from the soil. If large fractions of the surface are thus protected by foreign solids, sites under corrosion may become the exception whereas without the soil sites under corrosion would be the rule. As a consequence, the presence of soil or clay in the system may lead to that a certain amount of oxidant causes deeper corrosion attacks than would be the case without soil or clay in the system.

8 References

1-1 **Taxén, C.**

Pitting Corrosion of Copper- An Equilibrium Mass Transport Study, 13:th International Corrosion Conference, 25-29 Nov. 1996, Melbourne Australia, Paper No 141

2-1 **Puigdomenech, I.**

Personal Communication.

Later published as:

Puigdomenech, I. and Taxén, C.

Thermodynamic data for copper. Implications for the corrosion of copper under repository conditions, SKB Technical Report TR-00-13 (2000).

2-2 **National Institute For Standards And Testing**

Standard Reference Database 46 Version 3.0, Critically Selected Stability Constants Of Metal Complexes

2-3 **Woods, T. L. and Garrels, R. M.**

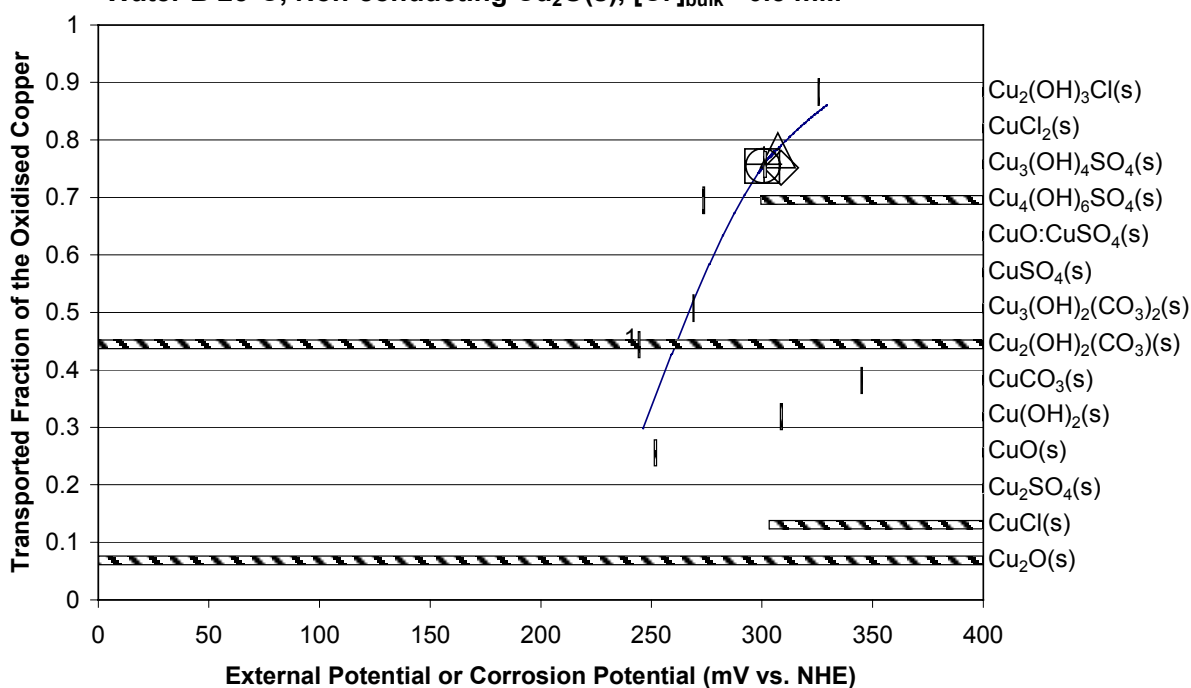
Phase Relations of some Cupric Hydroxy Minerals, Economic Geology **81** (1986) pp 1989-2007

9 Appendix 1. Selected result details for 25°C

Page No.	pH	Total Chloride (mM)	Total Sulphate (mM)	Total Carbonate (mM)	Others
A2	7.0	0.5	4.0	1.2	Sensitivity Analysis
A3					Details
A4	7.0	1.0	4.0	1.2	
A5	7.0	2.0	4.0	1.2	
A6					Details
A7	7.0	4.0	4.0	1.2	
A8	7.0	8.0	4.0	1.2	
A9					Details
A10	7.0	16.0	4.0	1.2	
A11	7.0	32.0	4.0	1.2	
A12					Details
A13	7.0	64.0	4.0	1.2	
A4	7.0	128.0	4.0	1.2	
A15					Details
A16	7.0	256	4.0	1.2	
A17	7.0	512.0	4.0	1.2	Sensitivity Analysis
A18					Details
A19	7.0	32.0	4.0	1.2	High [O ₂]
A20					Details
A21	7.0	0.5	0.5	1.2	
A22	7.0	1.0	1.0	1.2	
A23	7.0	0.5	0.5	1.2	Medium High [O ₂]
A24	8.0	1.0	4.0	1.2	

A25	9.0	1.0	4.0	1.2	
A26	7.0	0.5	0.5	1.2	Medium High [O ₂]
A27					Details
A28	7.0	0.5	0.5	1.2	Medium High [O ₂], High O ₂ flux
A29					Details

**Pitting Conditions as Function of the Potential,
Water B 25°C, Non-conducting Cu₂O(s), [Cl⁻]_{bulk} = 0.5 mM**



Water composition

Temperature °C	25	
pH	7.0	
Total Concentrations	moles/litre	mg/litre
Chloride	0.0005	17.7
Sulphate	0.0040	384.0
Carbonate (mg CO ₃ ²⁻)	0.0012	69.0
Calcium	0.0005	21.6
Sodium	0.0086	197.1
Copper	1E-12	6.3E-08
Oxygen	5E-06	0.2

Error analysis

Symbol

lg k for Cu₂O(s) increased

0.1 unit to

0.8445

*lg k* for CuCl₂⁻ increased

0.3 unit to

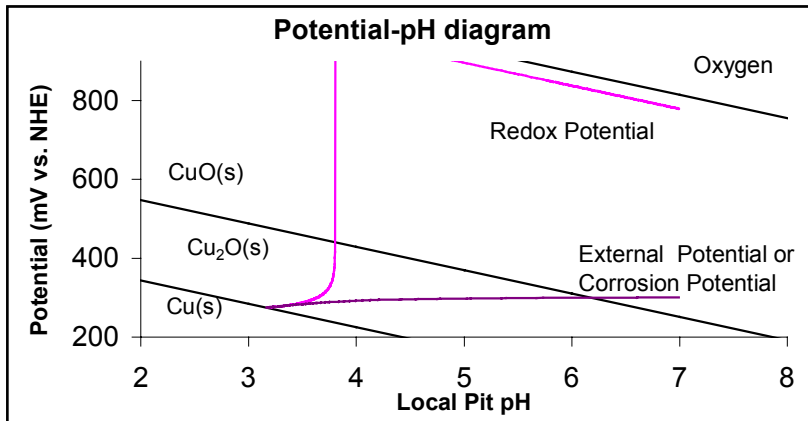
5.988

*lg k* for CuSO₄(aq) increased

0.3 unit to

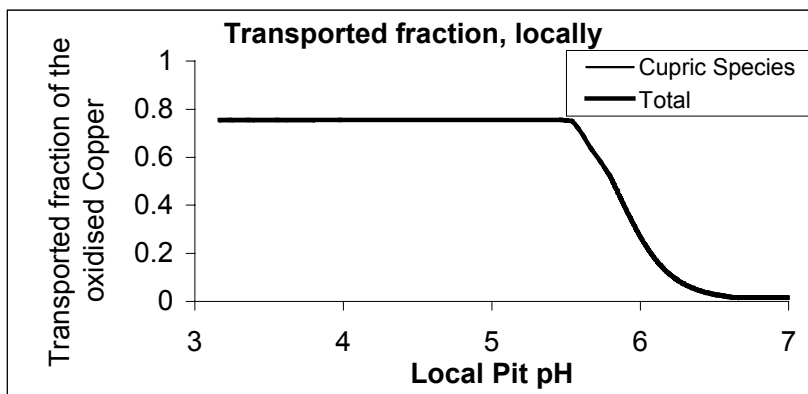
2.611

*D* for all aqueous cuprous species increased by a factor of 2

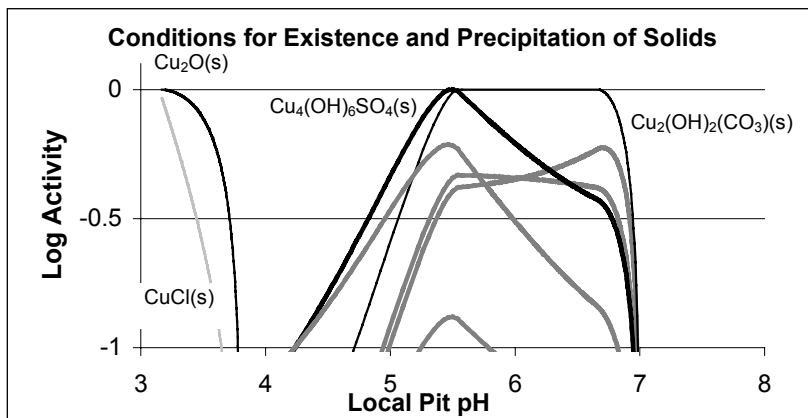


Figures corresponding to the conditions marked with a ring in the diagram on the previous page. Total chloride concentration in the bulk 0.5 mM.

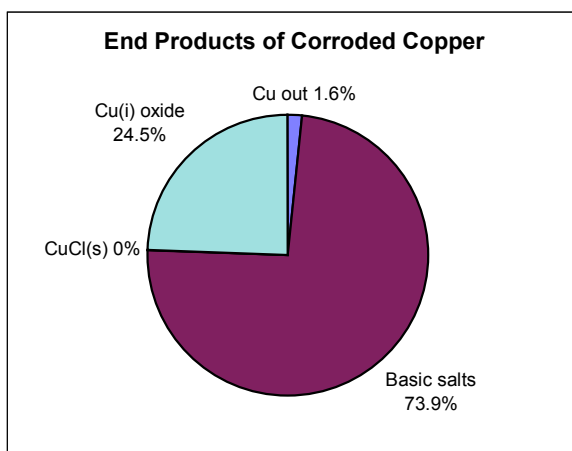
Representation of a corrosion pit in a potential pH-diagram where the relative stability regions for copper metal and the oxides are indicated.



The fraction of the oxidised copper transported as aqueous species as a function of the local pH in and around the pit.

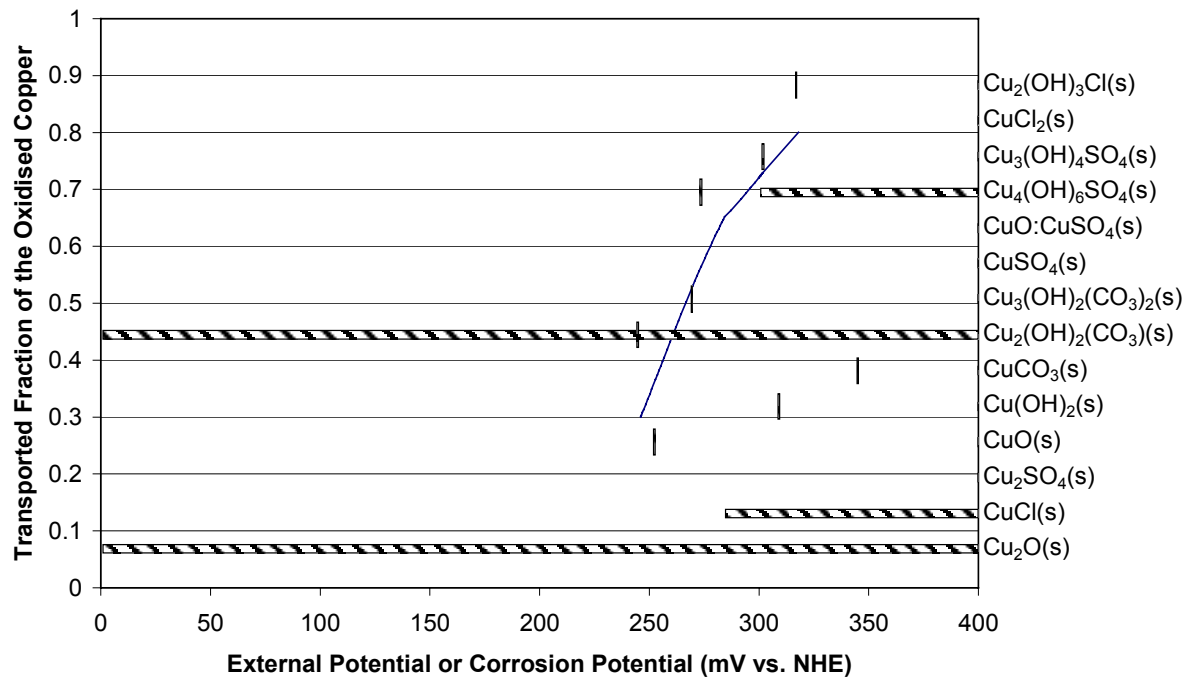


A plot of the calculated activity of the solids considered as function of the local pH.



A diagram showing the end distribution of the corroded copper.

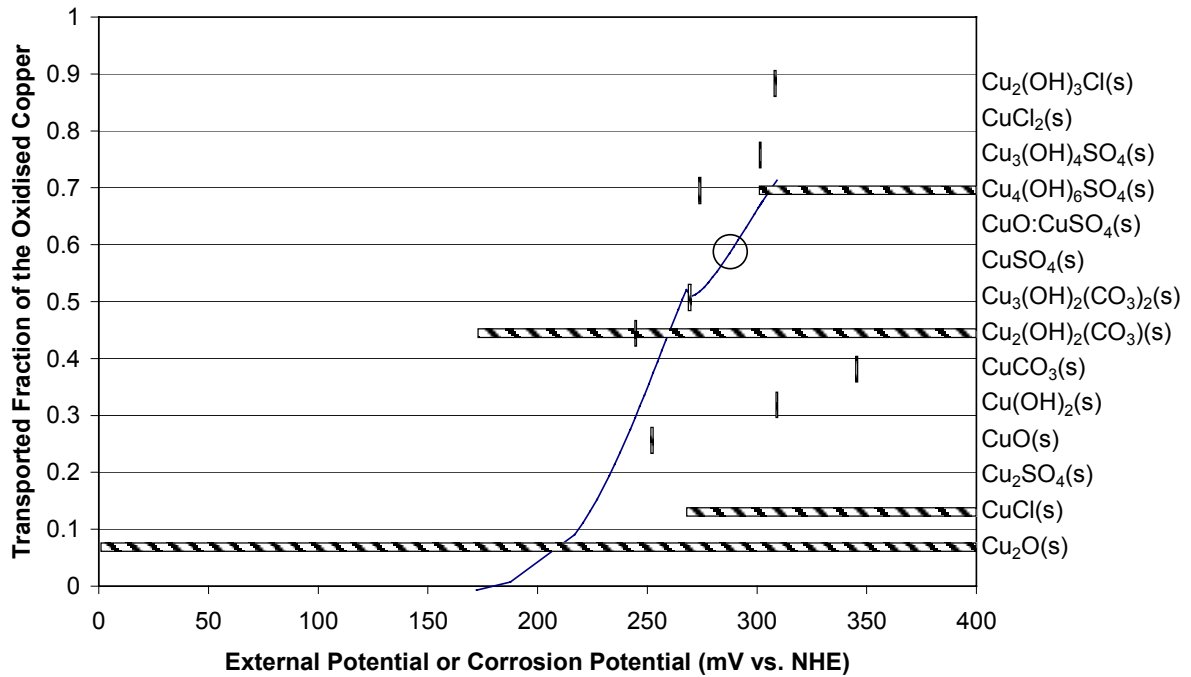
**Pitting Conditions as Function of the Potential,
Water B 25°C, Non-conducting Cu₂O(s), [Cl⁻]_{bulk} =1 mM**



Water composition

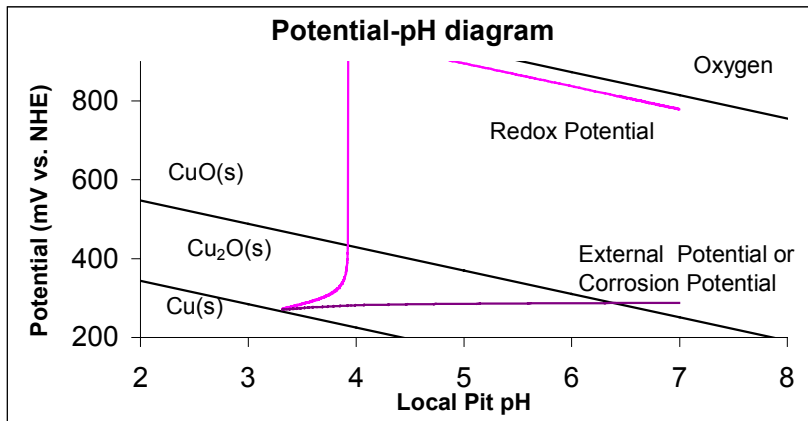
Temperature °C	25	
pH	7.0	
Total Concentrations	moles/litre	mg/litre
Chloride	0.0010	35.5
Sulphate	0.0040	384.0
Carbonate (mg CO ₃ ²⁻)	0.0012	69.0
Calcium	0.0005	21.6
Sodium	0.0091	208.6
Copper	1E-12	6.3E-08
Oxygen	5E-06	0.2

**Pitting Conditions as Function of the Potential,
Water B 25°C, Non-conducting Cu₂O(s), [Cl⁻]_{bulk} =2 mM**



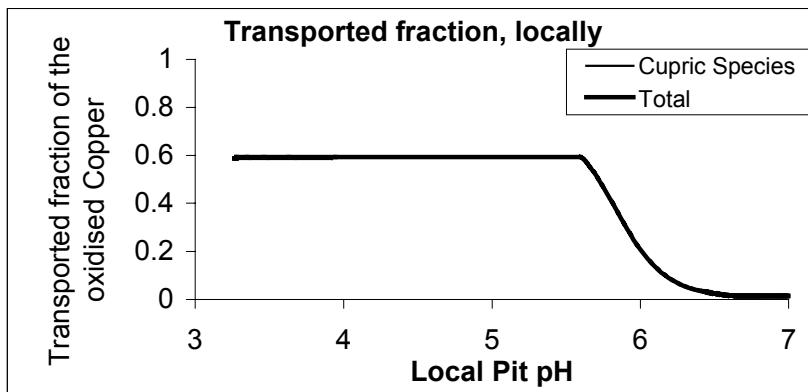
Water composition

Temperature °C	25	
pH	7.0	
Total Concentrations	moles/litre	mg/litre
Chloride	0.0020	70.9
Sulphate	0.0040	384.0
Carbonate (mg CO ₃ ²⁻)	0.0012	69.0
Calcium	0.0005	21.6
Sodium	0.0101	231.6
Copper	1E-12	6.3E-08
Oxygen	5E-06	0.2

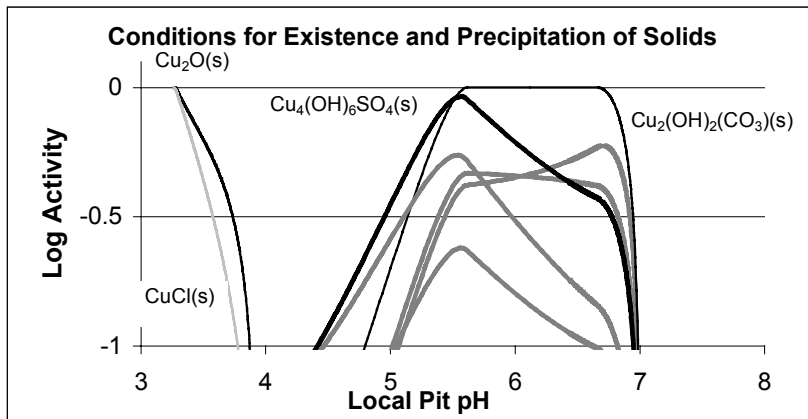


Figures corresponding to the conditions marked with a ring in the diagram on the previous page. Total chloride concentration in the bulk 2.0 mM.

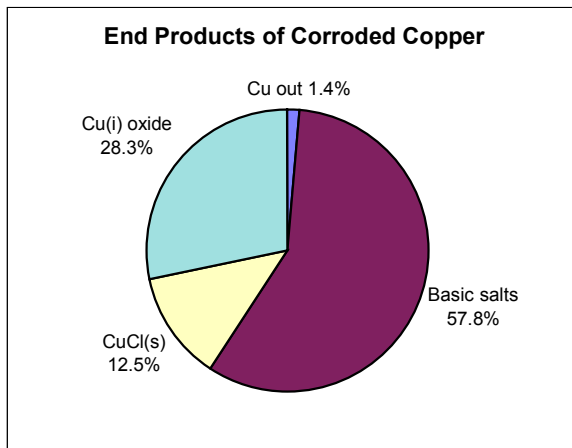
Representation of a corrosion pit in a potential pH-diagram where the relative stability regions for copper metal and the oxides are indicated.



The fraction of the oxidised copper transported as aqueous species as a function of the local pH in and around the pit.

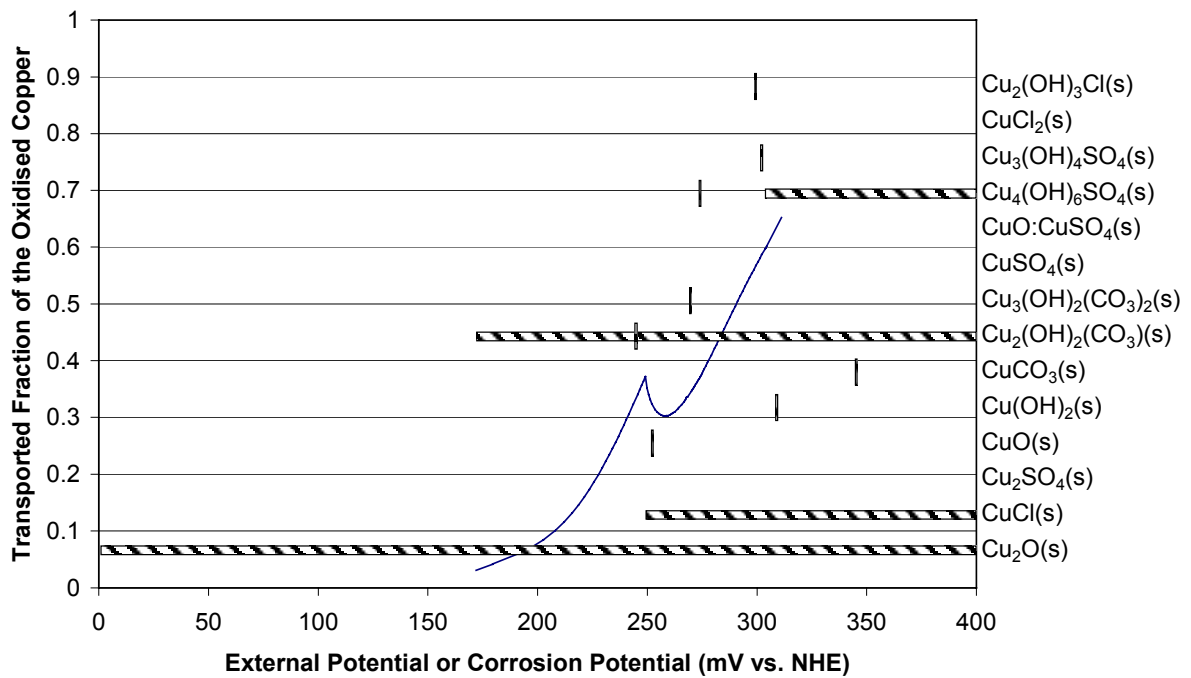


A plot of the calculated activity of the solids considered as function of the local pH.



A diagram showing the end distribution of the corroded copper.

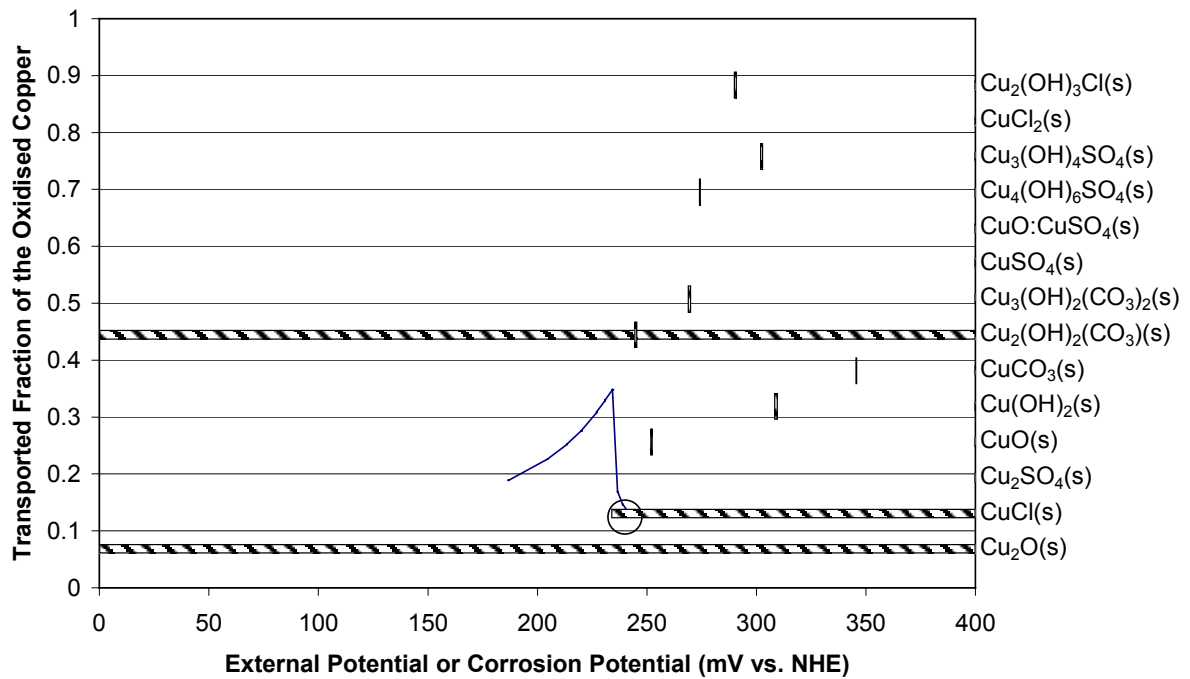
**Pitting Conditions as Function of the Potential,
Water B 25°C, Non-conducting Cu₂O(s), [Cl]_{bulk} =4 mM**



Water composition

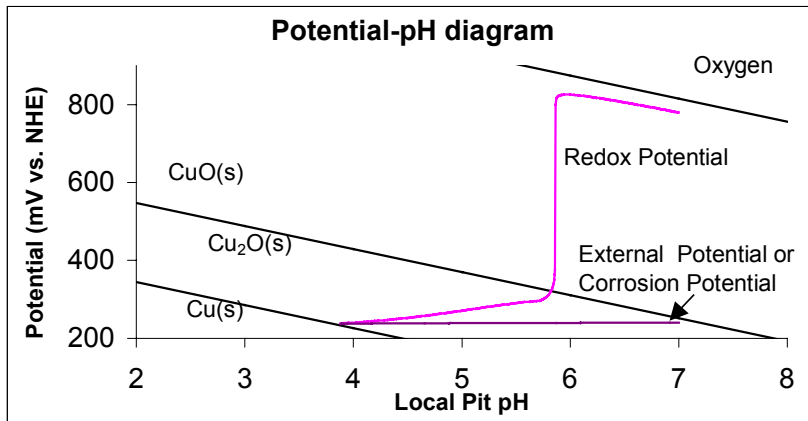
Temperature °C	25	
pH	7.0	
Total Concentrations	moles/litre	mg/litre
Chloride	0.0040	141.8
Sulphate	0.0040	384.0
Carbonate (mg CO ₃ ²⁻)	0.0012	69.0
Calcium	0.0005	21.6
Sodium	0.0121	277.6
Copper	1E-12	6.3E-08
Oxygen	5E-06	0.2

**Pitting Conditions as Function of the Potential,
Water B 25°C, Non-conducting Cu₂O(s), [Cl⁻]_{bulk} =8 mM**



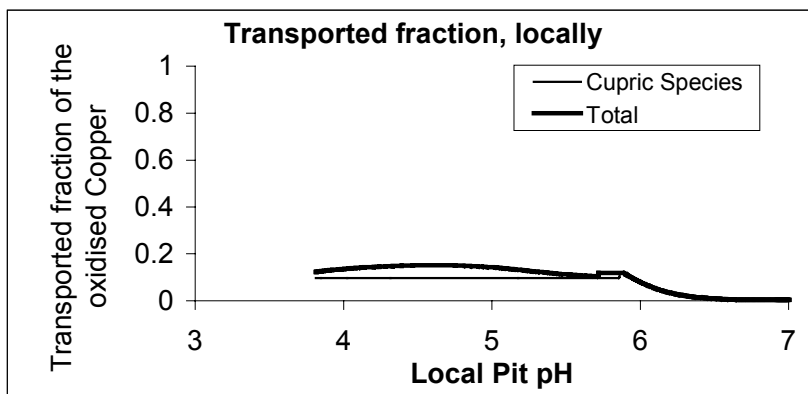
Water composition

Temperature °C	25	
pH	7.0	
Total Concentrations	moles/litre	mg/litre
Chloride	0.0080	283.6
Sulphate	0.0040	384.0
Carbonate (mg CO ₃ ²⁻)	0.0012	69.0
Calcium	0.0005	21.6
Sodium	0.0161	369.6
Copper	1E-12	6.3E-08
Oxygen	5E-06	0.2

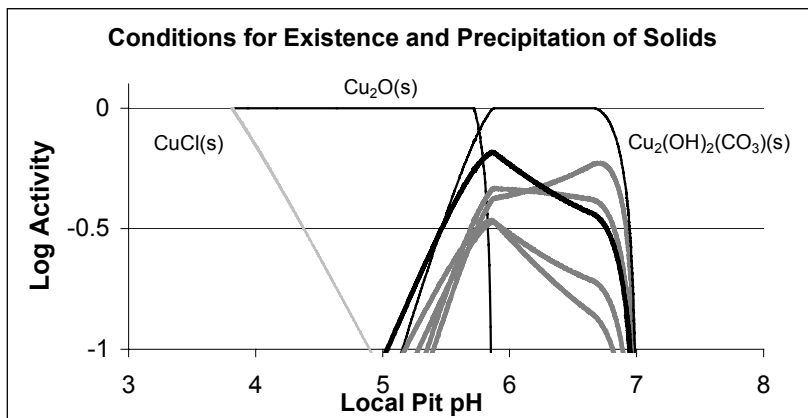


Figures corresponding to the conditions marked with a ring in the diagram on the previous page. Total chloride concentration in the bulk 8.0 mM.

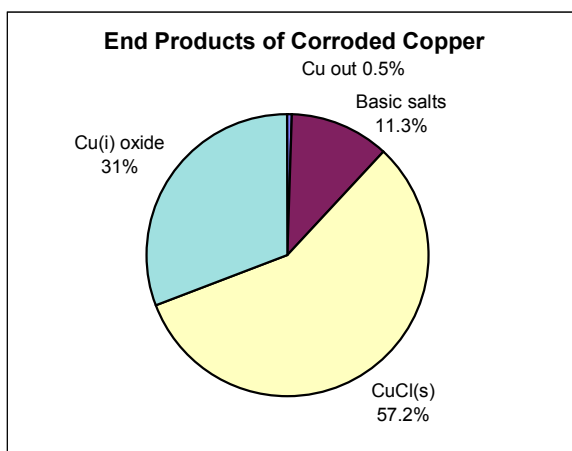
Representation of a corrosion pit in a potential pH-diagram where the relative stability regions for copper metal and the oxides are indicated.



The fraction of the oxidised copper transported as aqueous species as a function of the local pH in and around the pit.

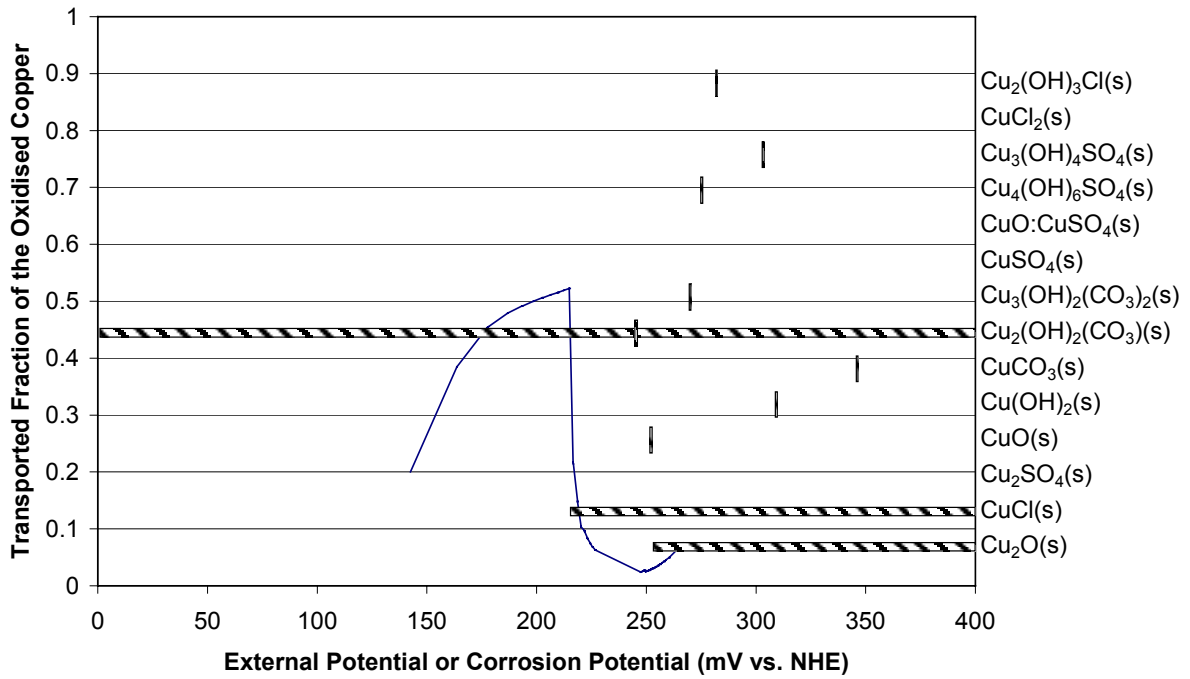


A plot of the calculated activity of the solids considered as function of the local pH.



A diagram showing the end distribution of the corroded copper.

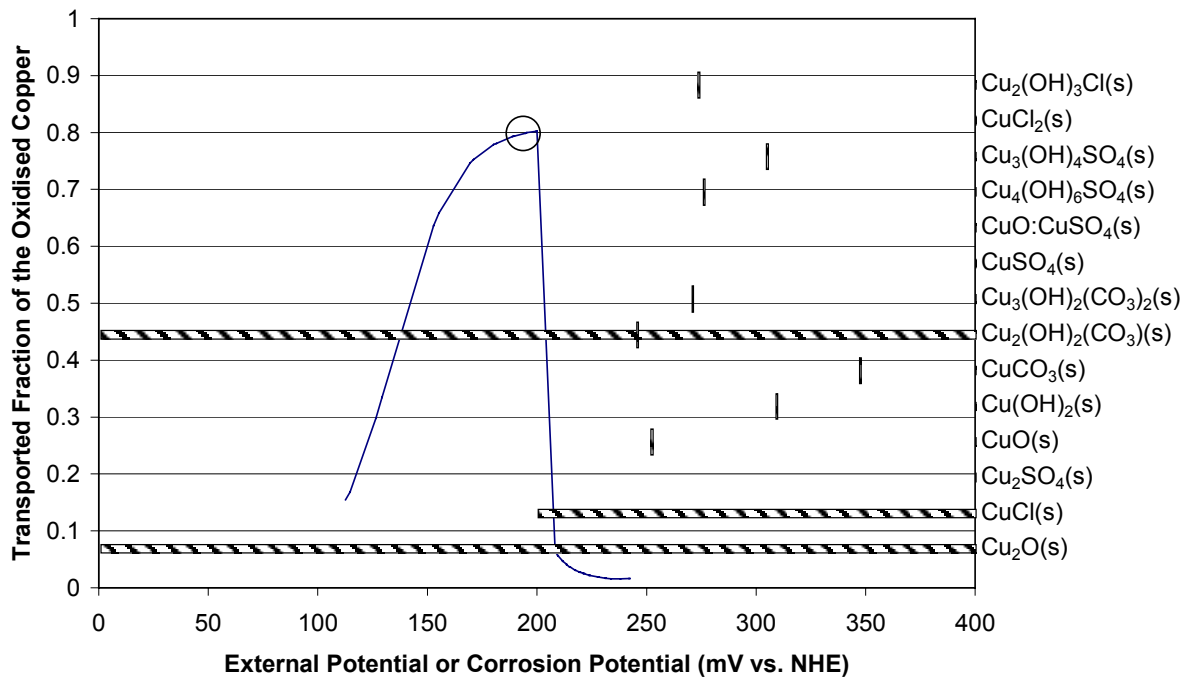
**Pitting Conditions as Function of the Potential,
Water B 25°C, Non-conducting Cu₂O(s), [Cl⁻]_{bulk} =16 mM**



Water composition

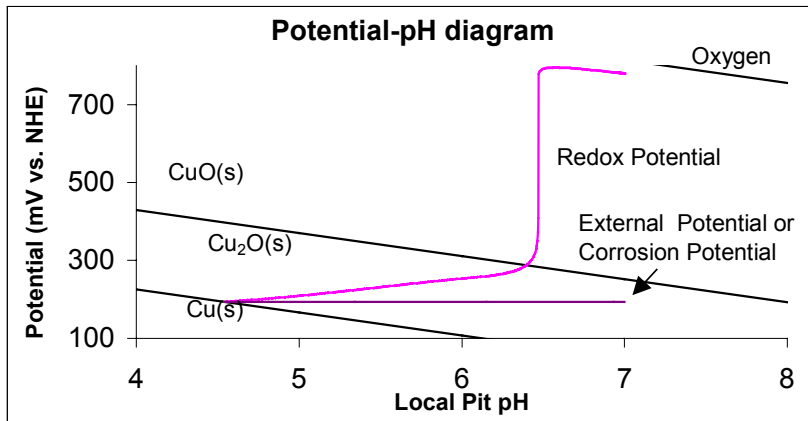
Temperature °C	25	
pH	7.0	
Total Concentrations	moles/litre	mg/litre
Chloride	0.0160	567.2
Sulphate	0.0040	384.0
Carbonate (mg CO ₃ ²⁻)	0.0012	69.0
Calcium	0.0005	21.6
Sodium	0.0241	553.6
Copper	1E-12	6.3E-08
Oxygen	5E-06	0.2

**Pitting Conditions as Function of the Potential,
Water B 25°C, Non-conducting Cu₂O(s), [Cl⁻]_{bulk} =32 mM**

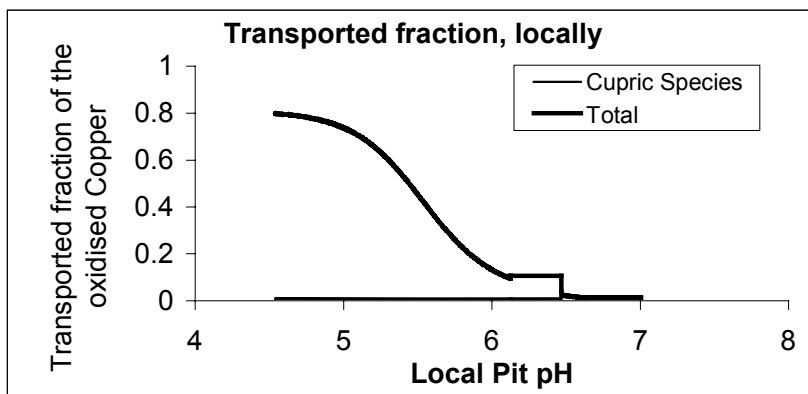


Water composition

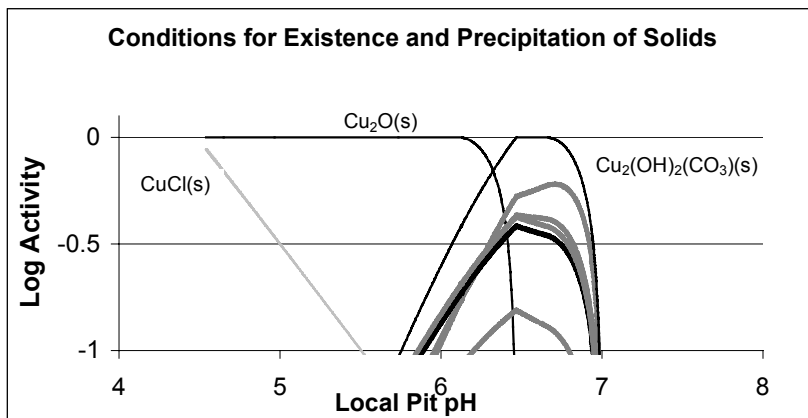
Temperature °C	25	
pH	7.0	
Total Concentrations	moles/litre	mg/litre
Chloride	0.0320	1134.5
Sulphate	0.0040	384.0
Carbonate (mg CO ₃ ²⁻)	0.0012	69.0
Calcium	0.0005	21.6
Sodium	0.0401	921.6
Copper	1E-12	6.3E-08
Oxygen	5E-06	0.2



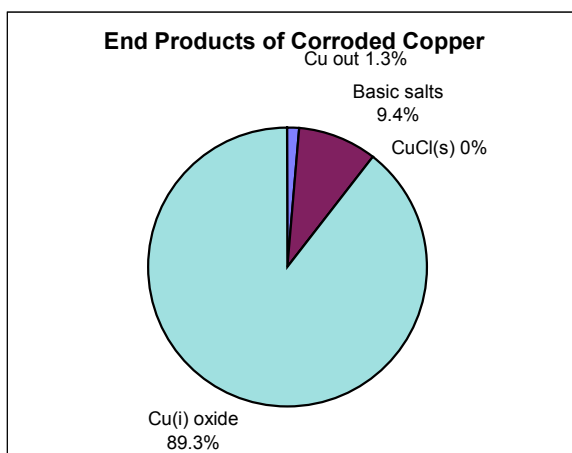
Figures corresponding to the conditions marked with a ring in the diagram on the previous page. Total chloride concentration in the bulk 32 mM.



Representation of a corrosion pit in a potential pH-diagram where the relative stability regions for copper metal and the oxides are indicated.



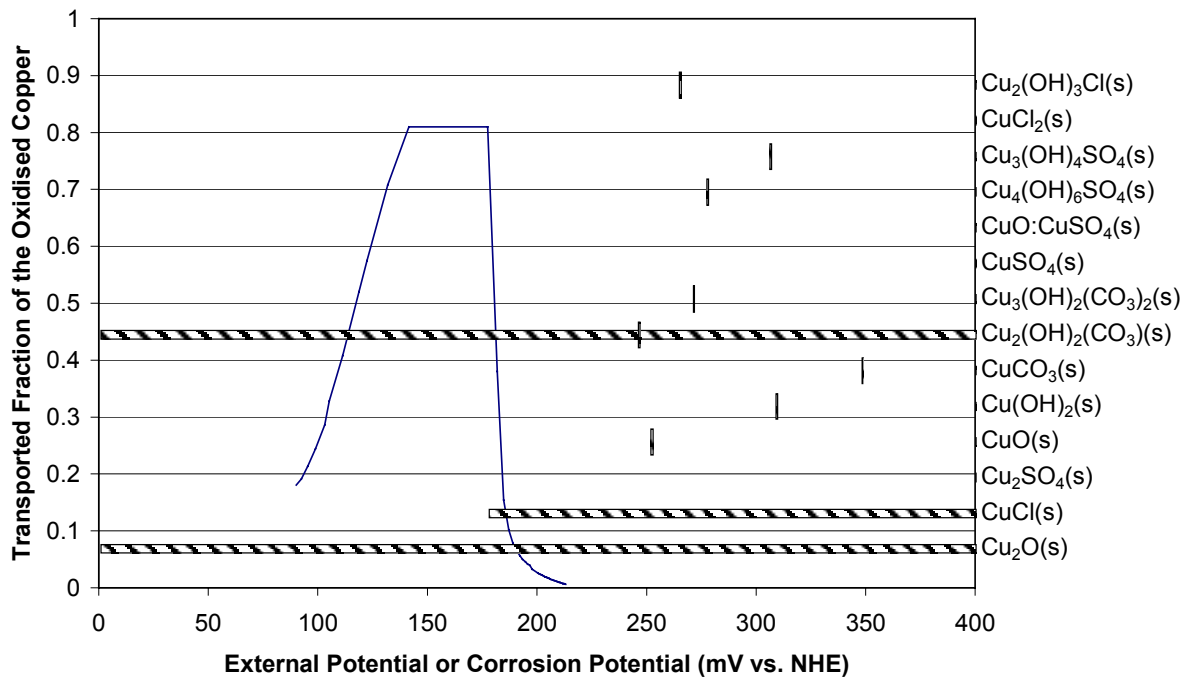
The fraction of the oxidised copper transported as aqueous species as a function of the local pH in and around the pit.



A plot of the calculated activity of the solids considered as function of the local pH.

A diagram showing the end distribution of the corroded copper.

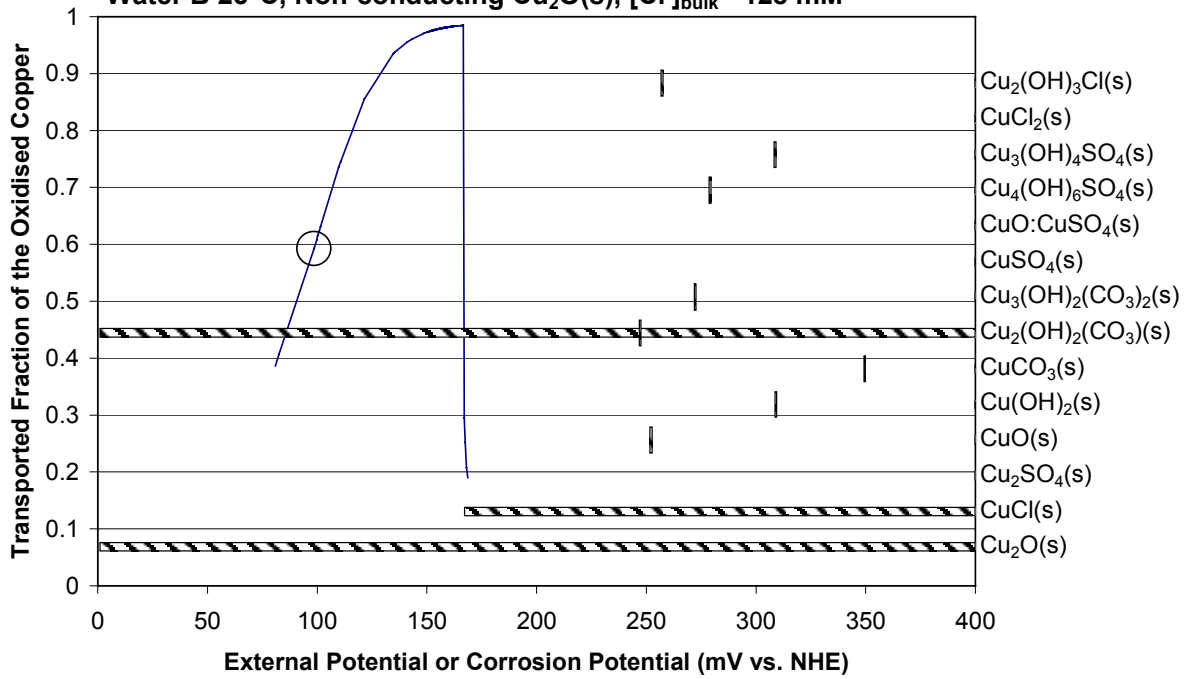
**Pitting Conditions as Function of the Potential,
Water B 25°C, Non-conducting Cu₂O(s), [Cl⁻]_{bulk} =64 mM**



Water composition

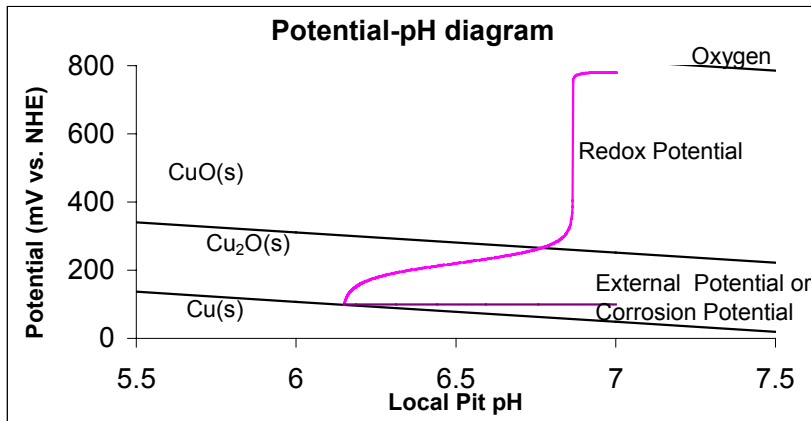
Temperature °C	25	
pH	7.0	
Total Concentrations	moles/litre	mg/litre
Chloride	0.0640	2269.0
Sulphate	0.0040	384.0
Carbonate (mg CO ₃ ²⁻)	0.0012	69.0
Calcium	0.0005	21.6
Sodium	0.0721	1657.6
Copper	1E-12	6.3E-08
Oxygen	5E-06	0.2

**Pitting Conditions as Function of the Potential,
Water B 25°C, Non-conducting Cu₂O(s), [Cl⁻]_{bulk} =128 mM**



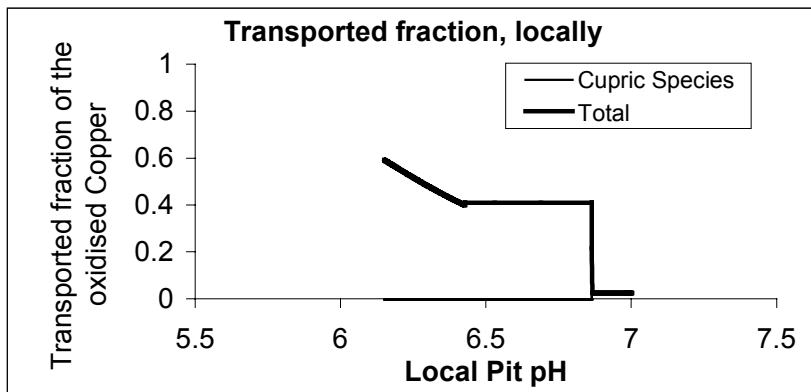
Water composition

Temperature °C	25	
pH	7.0	
Total Concentrations	moles/litre	mg/litre
Chloride	0.1280	4538.0
Sulphate	0.0040	384.0
Carbonate (mg CO ₃ ²⁻)	0.0012	69.0
Calcium	0.0005	21.6
Sodium	0.1361	3129.6
Copper	1E-12	6.3E-08
Oxygen	5E-06	0.2

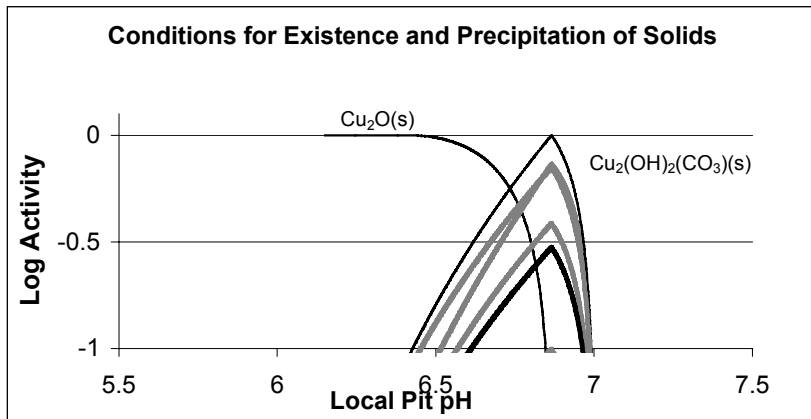


Figures corresponding to the conditions marked with a ring in the diagram on the previous page. Total chloride concentration in the bulk 128 mM.

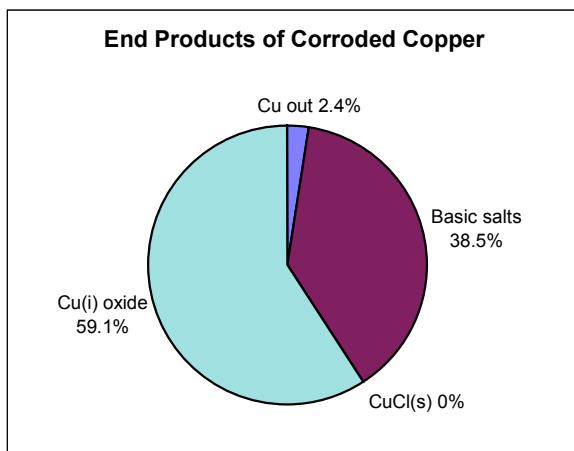
Representation of a corrosion pit in a potential pH-diagram where the relative stability regions for copper metal and the oxides are indicated.



The fraction of the oxidised copper transported as aqueous species as a function of the local pH in and around the pit.

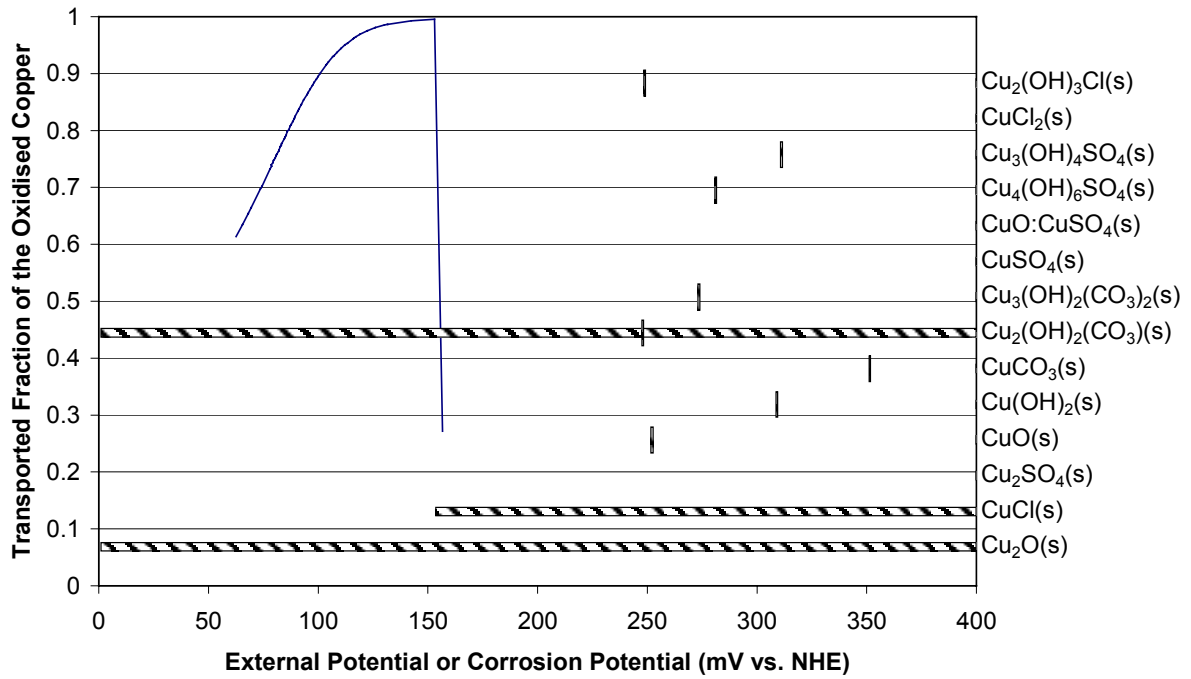


A plot of the calculated activity of the solids considered as function of the local pit pH.



A diagram showing the end distribution of the corroded copper.

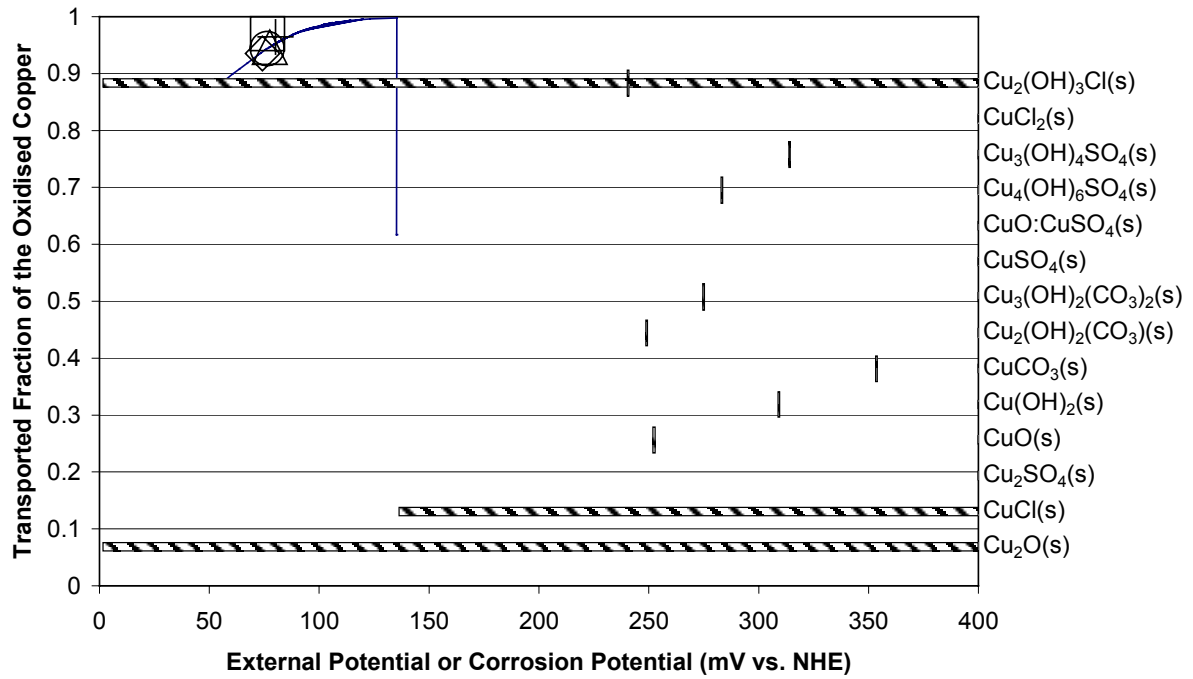
**Pitting Conditions as Function of the Potential,
Water B 25°C, Non-conducting Cu₂O(s), [Cl⁻]_{bulk} =256 mM**



Water composition

Temperature °C	25	
pH	7.0	
Total Concentrations	moles/litre	mg/litre
Chloride	0.2560	9076.0
Sulphate	0.0040	384.0
Carbonate (mg CO ₃ ²⁻)	0.0012	69.0
Calcium	0.0005	21.6
Sodium	0.2641	6073.6
Copper	1E-12	6.3E-08
Oxygen	5E-06	0.2

**Pitting Conditions as Function of the Potential,
Water B 25°C, Non-conducting Cu₂O(s), [Cl⁻]_{bulk} =512 mM**



Water composition

Temperature °C	25	
pH	7.0	
Total Concentrations	moles/litre	mg/litre
Chloride	0.5120	18151.9
Sulphate	0.0040	384.0
Carbonate (mg CO ₃ ²⁻)	0.0012	69.0
Calcium	0.0005	21.6
Sodium	0.5201	11961.6
Copper	1E-12	6.3E-08
Oxygen	5E-06	0.2

Error analysis

Symbol

lg k for $\text{Cu}_2\text{O}(\text{s})$ increased 0.1 unit to 0.8445



lg k for CuCl_2^- increased 0.3 unit to 5.988

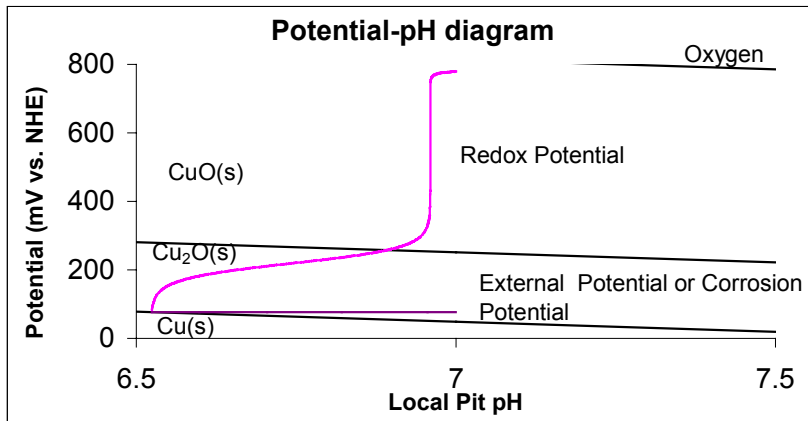


lg k for $\text{CuSO}_4(\text{aq})$ increased 0.3 unit to 2.611



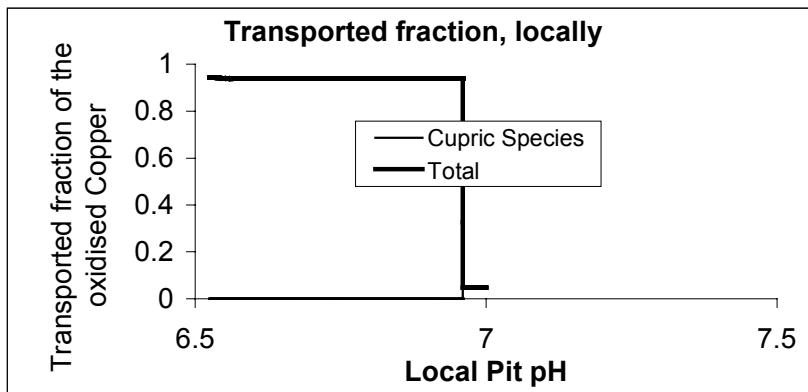
D for all aqueous cuprous species increased by a factor of 2



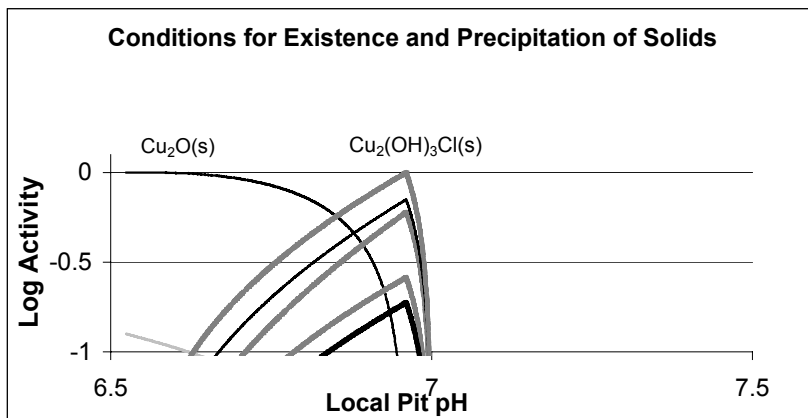


Figures corresponding to the conditions marked with a ring in the diagram on the previous page. Total chloride concentration in the bulk 512 mM.

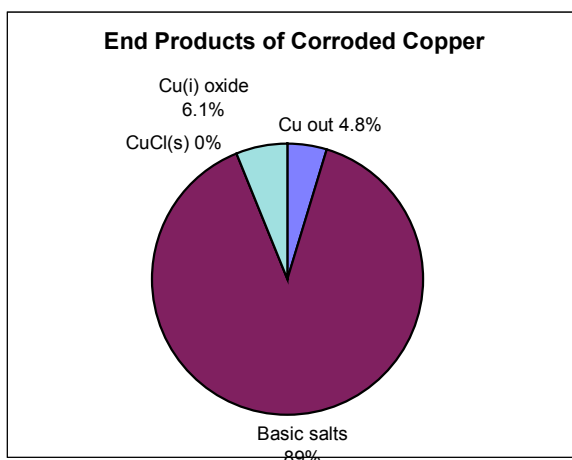
Representation of a corrosion pit in a potential pH-diagram where the relative stability regions for copper metal and the oxides are indicated.



The fraction of the oxidised copper transported as aqueous species as a function of the local pH in and around the pit.

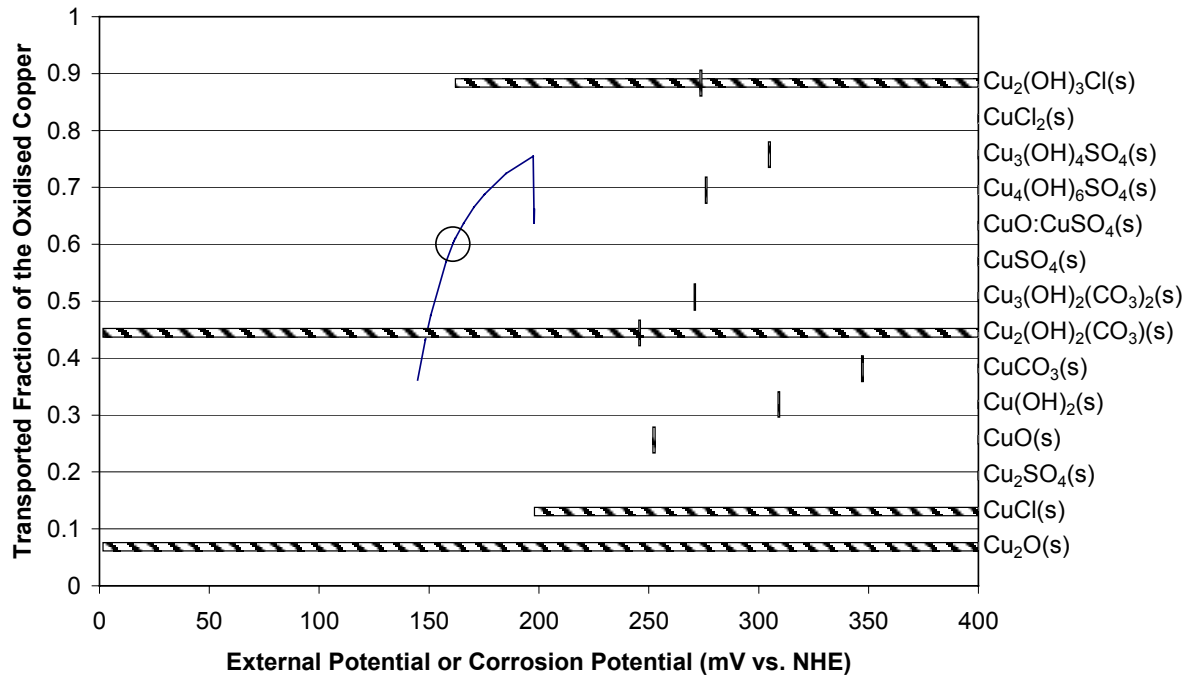


A plot of the calculated activity of the solids considered as function of the local pH.



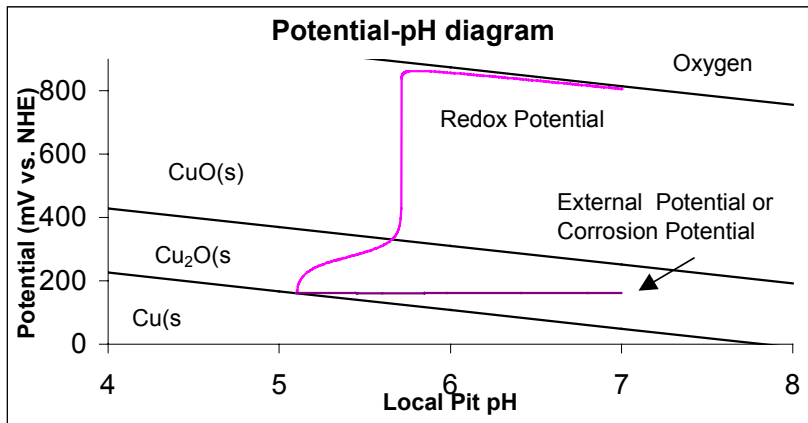
A diagram showing the end distribution of the corroded copper.

**Pitting Conditions as Function of the Potential,
Water B 25°C, Non-conducting Cu₂O(s), [Cl⁻]_{bulk} =32 mM**



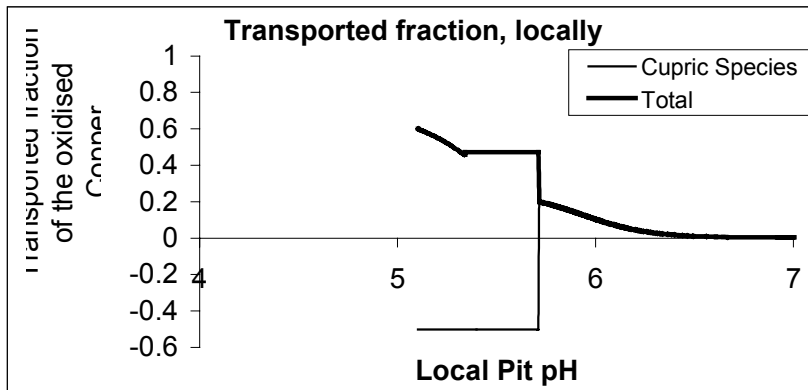
Water composition

Temperature °C	25	
pH	-7.0	
Total Concentrations	moles/litre	mg/litre
Chloride	0.0320	1134.5
Sulphate	0.0040	384.0
Carbonate (mg CO ₃ ²⁻)	0.0012	69.0
Calcium	0.0005	21.6
Sodium	0.0401	921.6
Copper	1.0E-12	6.3E-08
Oxygen	3.2E-4	10.2

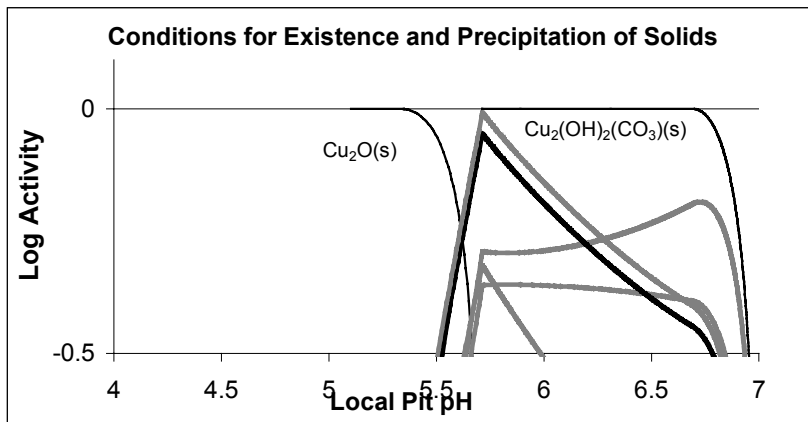


Figures corresponding to the conditions marked with a ring in the diagram on the previous page. Total chloride concentration in the bulk 32 mM.

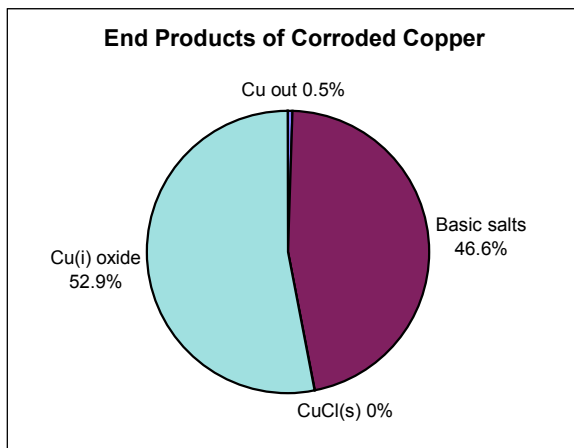
Representation of a corrosion pit in a potential pH-diagram where the relative stability regions for copper metal and the oxides are indicated.

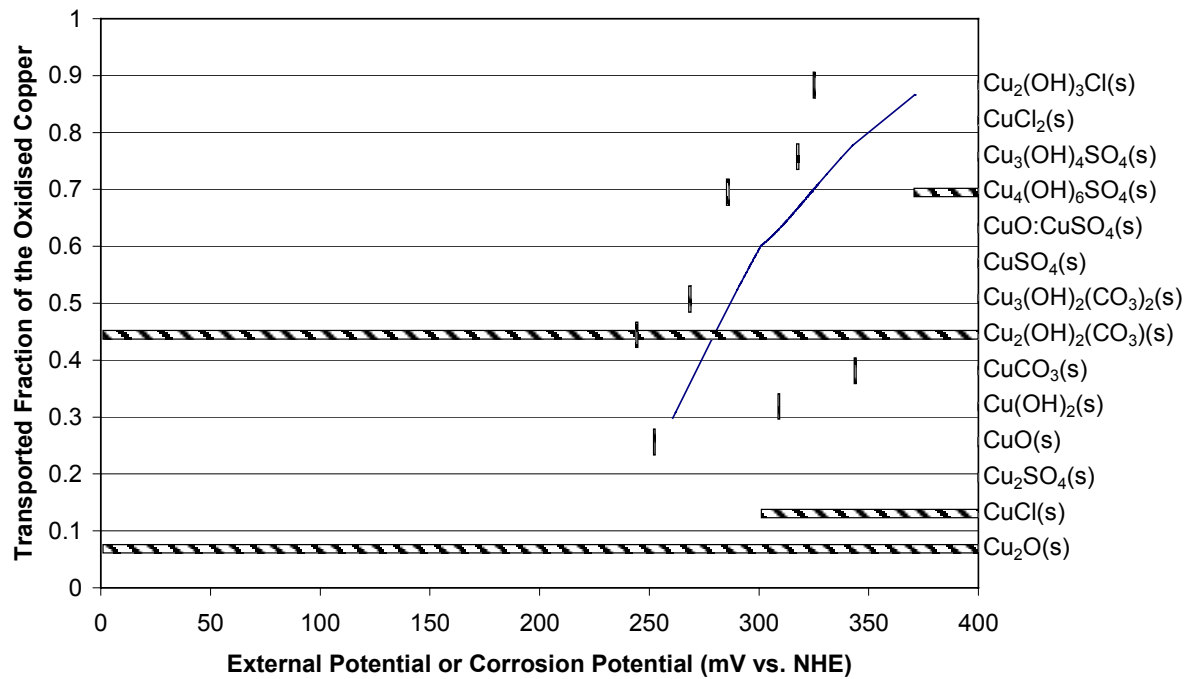


The fraction of the oxidised copper transported as aqueous species as a function of the local pH in and around the pit.



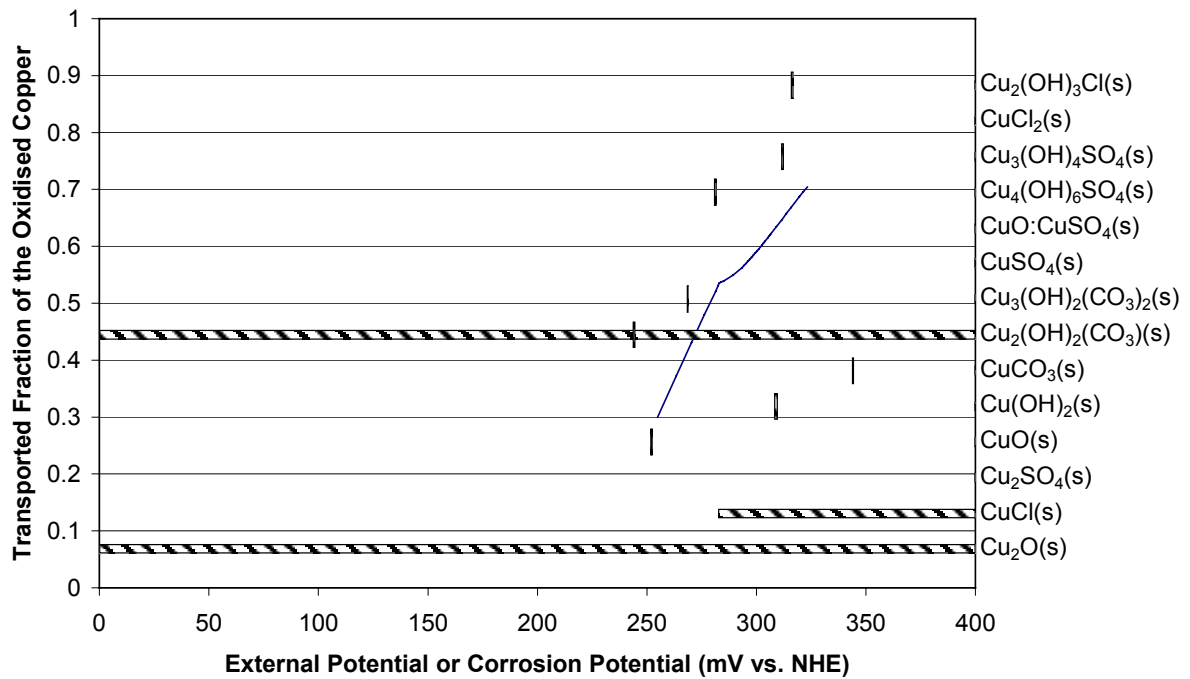
A plot of the calculated activity of the solids considered as function of the local pit pH.





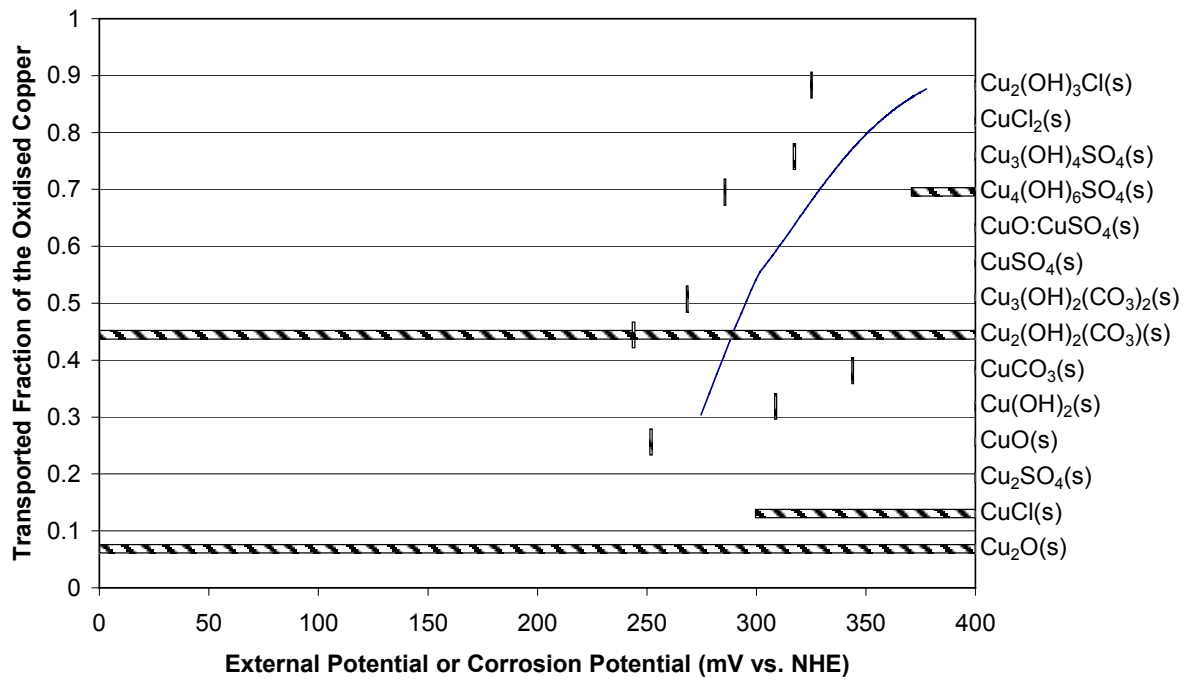
Water composition

Temperature °C	25	
pH	7.0	
Total Concentrations	moles/litr e	mg/litre
Chloride	0.0005	17.7
Sulphate	0.0005	48.0
Carbonate (mg CO ₃ ²⁻)	0.0012	69.0
Calcium	0.0005	21.6
Sodium	0.0016	36.1
Copper	1E-12	6.3E-08
Oxygen	5E-06	0.2



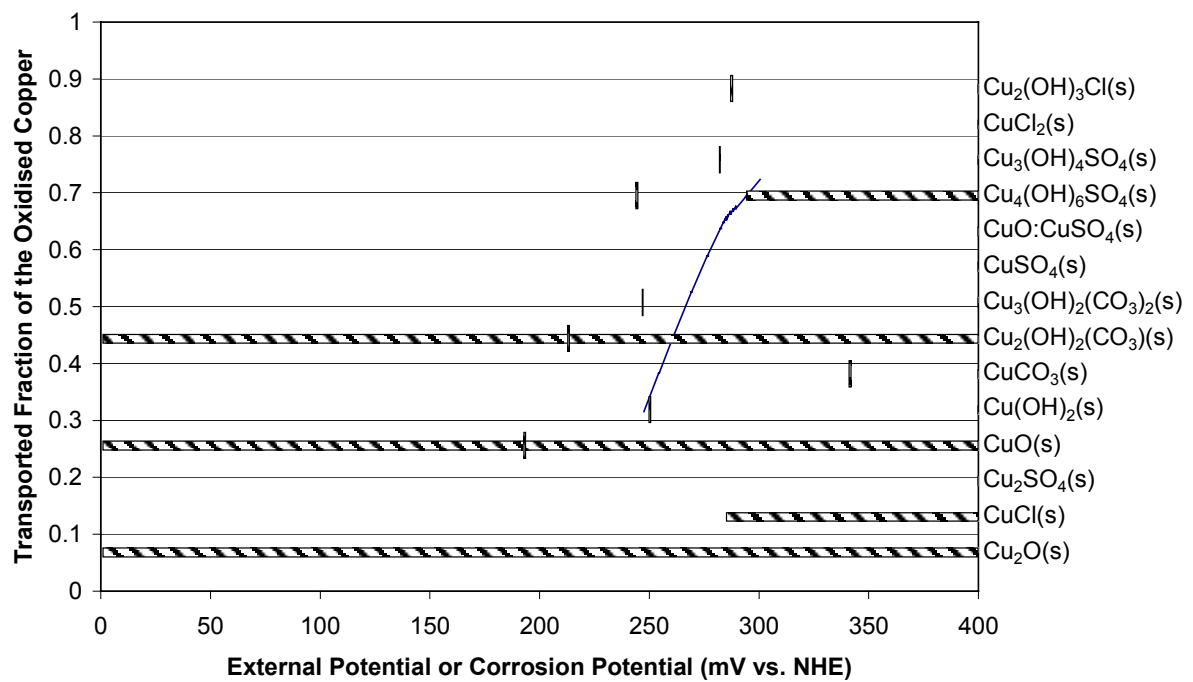
Water composition

Temperature °C	25	
pH	7.0	
Total Concentrations	moles/litre	mg/litre
Chloride	0.0010	35.5
Sulphate	0.0010	96.0
Carbonate (mg CO ₃ ²⁻)	0.0012	69.0
Calcium	0.0005	21.6
Sodium	0.0031	70.6
Copper	1E-12	6.3E-08
Oxygen	5E-06	0.2



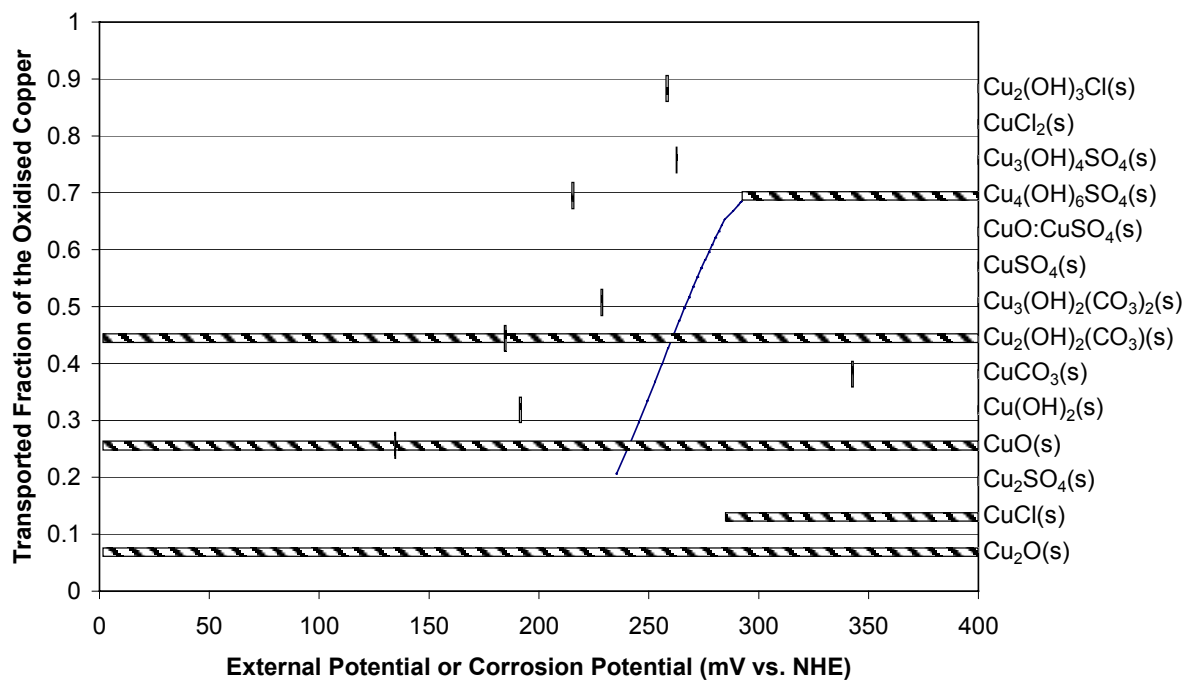
Water composition

Temperature °C	25	
pH	7.0	
Total Concentrations	moles/litre	mg/litre
Chloride	0.0005	17.7
Sulphate	0.0005	48.0
Carbonate (mg CO_3^{2-})	0.0012	69.0
Calcium	0.0005	21.6
Sodium	0.0016	36.1
Copper	1E-12	6.3E-08
Oxygen	8E-05	2.6



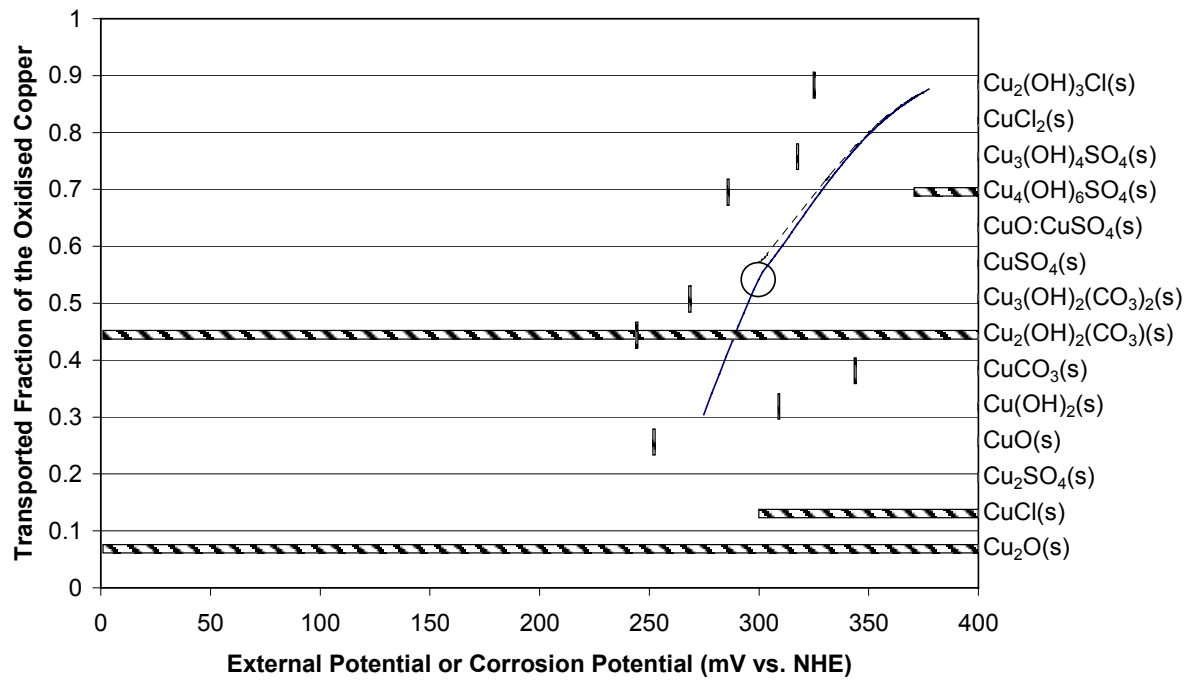
Water composition

Temperature °C	25	
pH	8.0	
Total Concentrations	moles/litr e	mg/litre
Chloride	0.0010	35.5
Sulphate	0.0040	384.0
Carbonate (mg CO ₃ ²⁻)	0.0012	69.0
Calcium	0.0005	21.6
Sodium	0.0091	208.6
Copper	1E-12	6.3E-08
Oxygen	5E-06	0.2



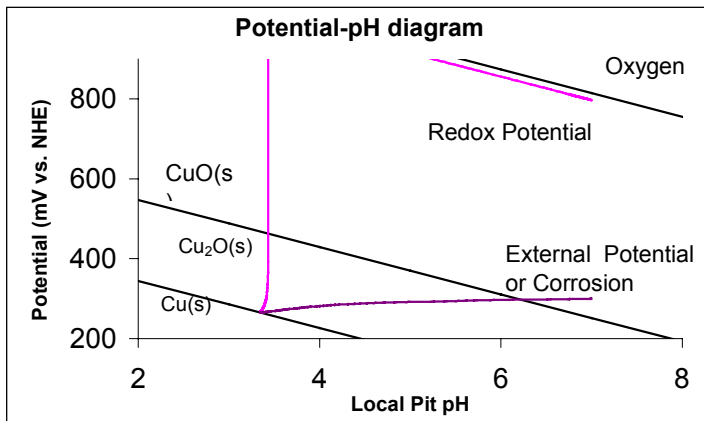
Water composition

Temperature °C	25	
pH	9.0	
Total Concentrations	moles/litr e	mg/litre
Chloride	0.0010	35.5
Sulphate	0.0040	384.0
Carbonate (mg CO ₃ ²⁻)	0.0012	69.0
Calcium	0.0005	21.6
Sodium	0.0091	208.6
Copper	1E-12	6.3E-08
Oxygen	5E-06	0.2



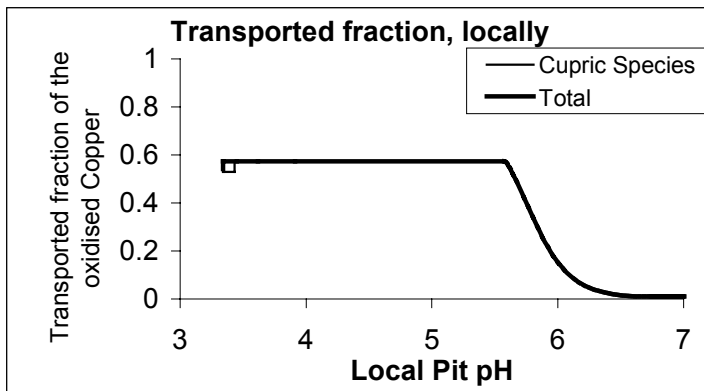
Water composition

Temperature °C	25	
pH	7.0	
Total Concentrations	moles/litr	mg/litre
	e	
Chloride	0.0005	17.7
Sulphate	0.0005	48.0
Carbonate (mg CO ₃ ²⁻)	0.0012	69.0
Calcium	0.0005	21.6
Sodium	0.0016	36.1
Copper	1E-12	6.3E-08
Oxygen	8E-05	2.6

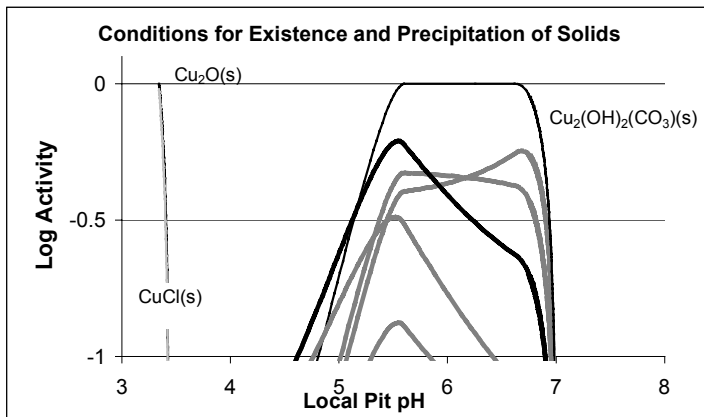


Figures corresponding to the conditions marked with a ring in the diagram on the previous page. Total chloride concentration in the bulk 0.5 mM.

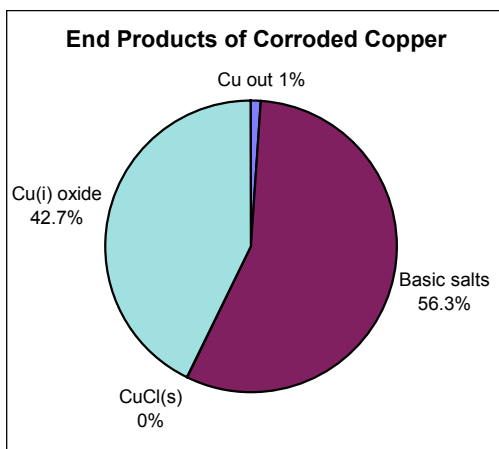
Representation of a corrosion pit in a potential pH-diagram where the relative stability regions for copper metal and the oxides are indicated.



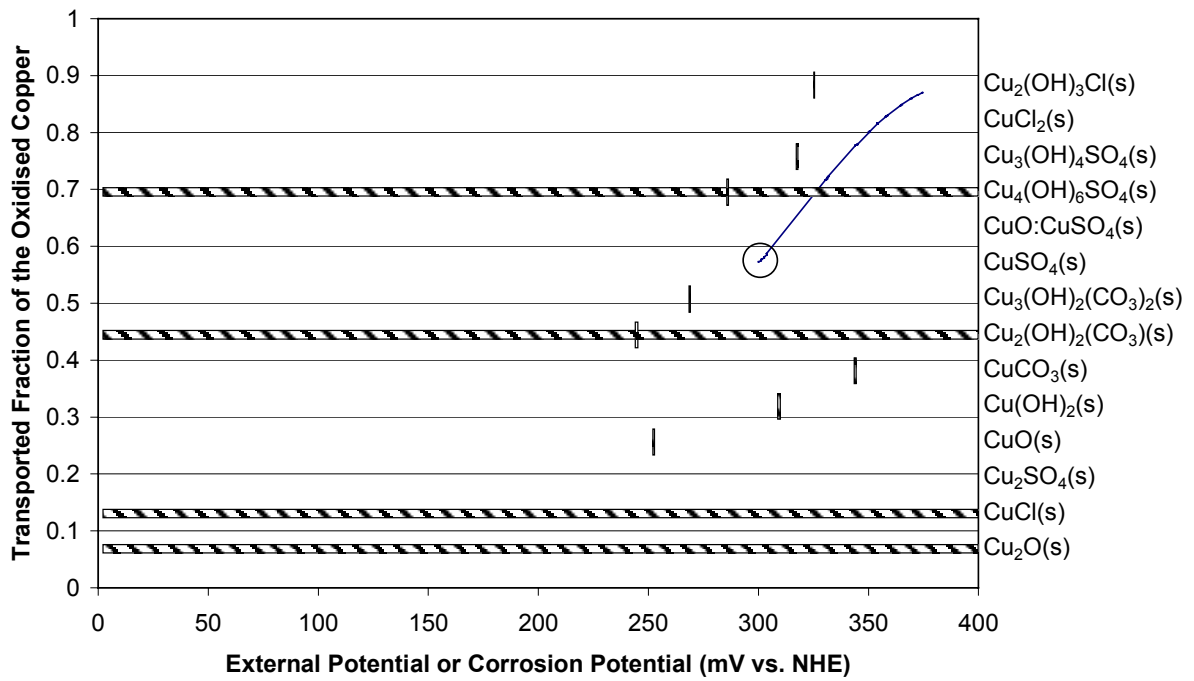
The fraction of the oxidised copper transported as aqueous species as a function of the local pH in and around the pit.



A plot of the calculated activity of the solids considered as function of the local pit pH.



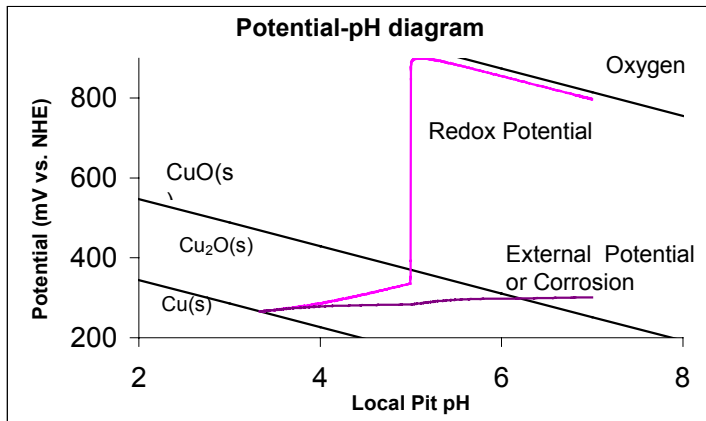
A diagram showing the end distribution of the corroded copper.



Water composition

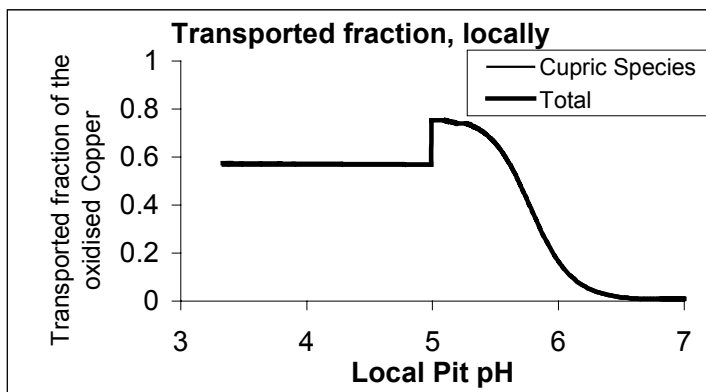
Temperature °C	25	
pH	7.0	
Total Concentrations	moles/litr e	mg/litre
Chloride	0.0005	17.7
Sulphate	0.0005	48.0
Carbonate (mg	0.0012	69.0

CO ₃ ²⁻)		
Calcium	0.0005	21.6
Sodium	0.0016	36.1
Copper	1E-12	6.3E-08
Oxygen	8E-05	2.6

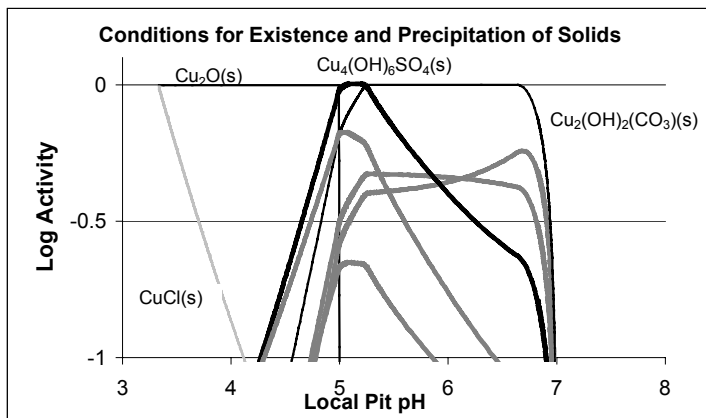


Figures corresponding to the conditions marked with a ring in the diagram on the previous page. Total chloride concentration in the bulk 0.5 mM.

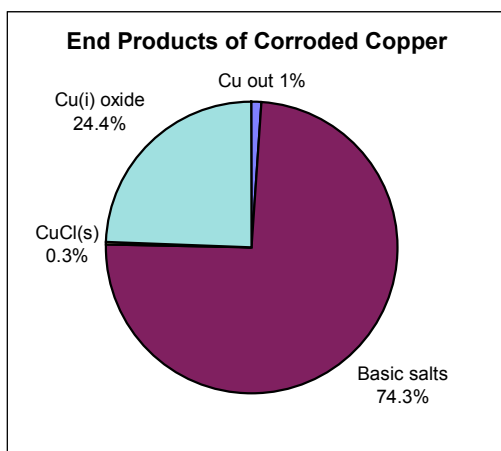
Representation of a corrosion pit in a potential pH-diagram where the relative stability regions for copper metal and the oxides are indicated.



The fraction of the oxidised copper transported as aqueous species as a function of the local pH in and around the pit.



A plot of the calculated activity of the solids considered as function of the local pit pH.



Figures corresponding to the conditions marked with a ring in the diagram on the previous page. Total chloride concentration in the bulk 0.5 mM.

Representation of a corrosion pit in a potential pH-diagram where the relative stability regions for copper metal and the oxides are indicated.

The fraction of the oxidised copper transported as aqueous species as a function of the local pH in and around the pit.

A plot of the calculated activity of the solids considered as function of the local pit pH.

